Bioorganic chemistry (Print) 2020; 105:104424, 1-16

(DOI: 10.1016/j.bioorg.2020.104424)

Novel [1,2,3]triazolo[4,5-d]pyrimidine derivatives containing hydrazone fragment as potent and selective anticancer agents

Chenhao Xu[a, 1], Wenjuan Zhou[a, b, 1], Guanjun Dong[a], Hui Qiao[a], Jiadi Peng[a], Pengfei Jia[a], Yuhao Li[a], Hongmin Liu[a], Kai Sun[a, *], Wen Zhao[a, *]

[a] State Key Laboratory of Esophageal Cancer Prevention and Treatment; Key Laboratory of Advanced Pharmaceutical Technology, Ministry of Education of China; Zhengzhou University School of Pharmaceutical Sciences and Institute of Drug Discovery & Development, Zhengzhou University, 100 Kexue Avenue, Zhengzhou, Henan, 450001, China

[b] Department of Pathology, Oslo University Hospital; Faculty of Medicine, University of Oslo, Oslo, 0379, Norway

[1]: Both authors contribute equally to this work.

[*]: These senior authors contribute equally to this work.

*Corresponding Authors: Zhao Wen, Ph.D and Sun Kai, Ph.D

State Key Laboratory of Esophageal Cancer Prevention and Treatment; Key Laboratory of Advanced Pharmaceutical Technology, Ministry of Education of China; Zhengzhou University School of Pharmaceutical Sciences and Institute of Drug Discovery & Development, Zhengzhou University, 100 Kexue Avenue, Zhengzhou, Henan, 450001, China

E-mail address: zhaowen100@139.com, kaisun@zzu.edu.cn.

Abstract: In this paper, based on molecular hybridization, a series of [1,2,3]triazolo[4,5-d]pyrimidine derivatives containing hydrazine was synthesized and their antiproliferative activities against 5 cancer cell lines (MGC-803, PC3, PC9, EC9706 and SMMC-7721) were evaluated. We found that most of them exhibited obvious growth inhibition effects on these tested cancer cells, especially compound **34** on PC3 cells (IC_{50} = 26.25±0.28 nM). Meanwhile, compound **34** displayed best selectivity on PC3, compared with the other cancer cell lines, as well as excellent selectivity towards normal cell lines (Het-1A, L02 and GES-1). Further investigations demonstrated that **34** could significantly inhibit PC3 cells' colony formation, increase cellular ROS content, suppress EGFR expression and induce apoptosis. Our findings indicate that **34** may serve as a novel lead compound for the discovery of more triazolopyrimidine derivatives with improved anticancer potency and selectivity.

Keywords: [1,2,3]triazolo[4,5-d]pyrimidine, Hydrazone, Anti-prostatic, ROS, Apoptosis, EGFR.

1. Introduction

Cancer, one of the hardest problems and a major public health problem worldwide, seriously threatens human life and social development. One in six people die of cancer every year worldwide and cancer burden is increasing year by year [1, 2]. Lung cancer is the most common cancer type in terms of both incidence and mortality [1, 2]. Prostate cancer has surpassed lung cancer as the most common in men [2, 3]. Liver cancer, esophageal cancer and gastric cancer all have a low survival rate less than 20% in the world [2, 4]. Although have found some highly effective medicines and treatment approaches, we still face a great challenge. Therefore, it is imperative to develop novel anticancer agents with more powerful potency, more significant selectivity and lower toxicity towards normal cells.

Purines as a basic element of all living organisms play a vital role in metabolism, energy transaction, nucleic acid synthesis and varieties of biochemical reactions [5]. Researchers have confirmed that purine derivatives were extensively applied to some diseases, such as cancer [6], viral [7], neuropsychiatric [8] and hypotensive [9]. Representative drugs are 6-mercaptopurine [10], 6-thioguanine [11] and 2-amino-6-alkyl thiopurine [12], which have been widely used for

treating leukemia and lymphoma. As the analogue of purines, [1,2,3]triazolo[4,5-d]pyrimidine derivatives recently have been reported to possess diverse and promising biological activities [13-15], especially for cancer treatment. For example, Compound **A** (Fig. 1) was reported to be an inhibitor of lysine specific demethylase 1 (LSD1) and showed strong antiproliferative activity against leukemia and lymphoma cell lines [16]. Compound **B** (Fig. 1) was found as a dual PI3K/mTOR inhibitor with low nanomolar potency against some cancer cell lines [17].

On the other hand, hydrazone scaffold is considered as a privileged structure, due to its extensive applications, like medicinal agents, agrochemicals and functional materials [18]. The skeleton, represented by the fusion between the amide and the imine subunits, provides pharmacophoric points to include hydrogen-bond acceptor and donor sites and to perform interaction with a wide range of amino-acid residues. The hydrazone derivatives have been shown significant pharmacological activities, such as antibacterial [19], antitumor [20], antiviral [21] and anti-inflammatory [22]. Furthermore, two representative compounds **C** and **D** (Fig. 1), which had been found as antitumor agents possessed potent and selective inhibitory effects on histone deacetylase-6/8 (HDAC 6/8) [23] and LSD1 [24], respectively.

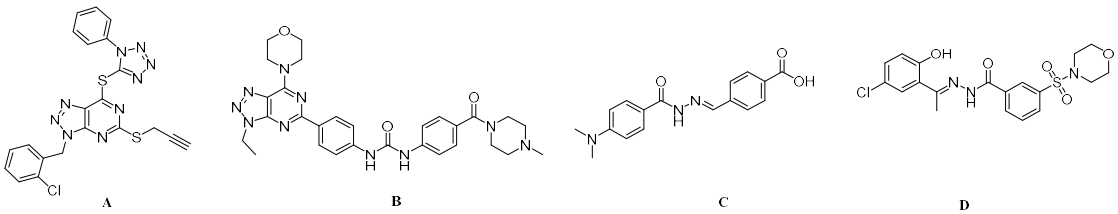

Fig. 1 Some previously reported [1,2,3]triazolo[4,5-d]pyrimidine and hydrazone derivatives as antiproliferative agents.

Recently, our group has reported several articles about the design and synthesis of [1,2,3]triazolo[4,5-d]pyrimidine-based [25-27] and hydrazone-based derivatives [28, 29], which displayed potent antiproliferative activity. Among them, compound **E** as [1,2,3]triazolo[4,5-d]pyrimidine derivatives [27] and compound **F** as hydrazone derivatives[29] (Fig. 2) exhibited highly potent inhibition against PC3 with IC_{50} values of 13.32 μM and 2.33 μM, respectively. Structure-guided molecular hybridization has been widely used in new drug design in the past years. New hybrid molecules may strengthen pharmacological effects, reduce toxicity or improve selectivity [30, 31]. Based on structure-guided molecular hybridization,

inspired by compounds **E** and **F**, we herein combine both [1,2,3]triazolo[4,5-d]pyrimidine and hydrazone scaffolds, designed and synthesized a series of novel compounds expecting to discover compounds with more powerful activity and better selectivity (Fig. 2). All these compounds were evaluated for their potential cytotoxic effects against five human cancer cell lines (MGC-803, PC3, EC9706 and SMMC-7721) to explore selectivity between PC3 and other cancer cell lines. The results showed that **34** possessed the most powerful potency against PC3 and best selectivity between PC3 and other four cancer cell lines. Therefore, we further investigated the effects of compound **34** on the cell proliferation, apoptosis, cellular ROS level and EGFR expression level.

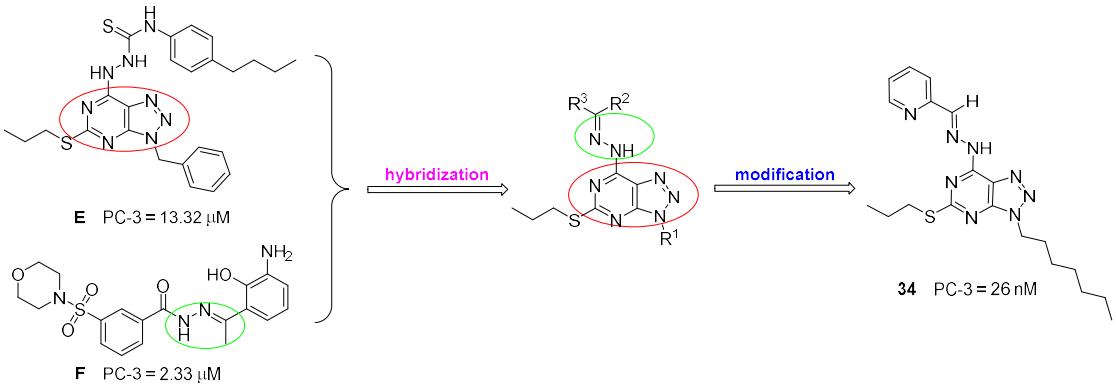

Fig. 2 Design of novel [1,2,3]triazolo[4,5-d]pyrimidine derivatives containing hydrazone scaffold.

2. Results and discussion

2.1 Chemistry

The general route for the synthesis of target compounds **5~34** is illustrated in scheme 1. The intermediates **2a~k** were prepared via the substitution reaction of compound **1** with some appropriate amines and triethylamine in ethanol followed by extraction with ethyl acetate, similar to the previously reported procedure in our group [27]. Compounds **3a~k** were synthesized by nitrification of **2a~k**, which was conducted with acetic acid in the presence of $NaNO_2$ under an ice bath. Next, the hydrazine hydrate was slowly added to **3a~k** in ethanol. After filtration and drying, compounds **4a~k** were obtained. Finally, target compounds **5~34** were readily generated by refluxing **4a~k** with appropriate aromatic aldehyde and ketone in

ethanol.

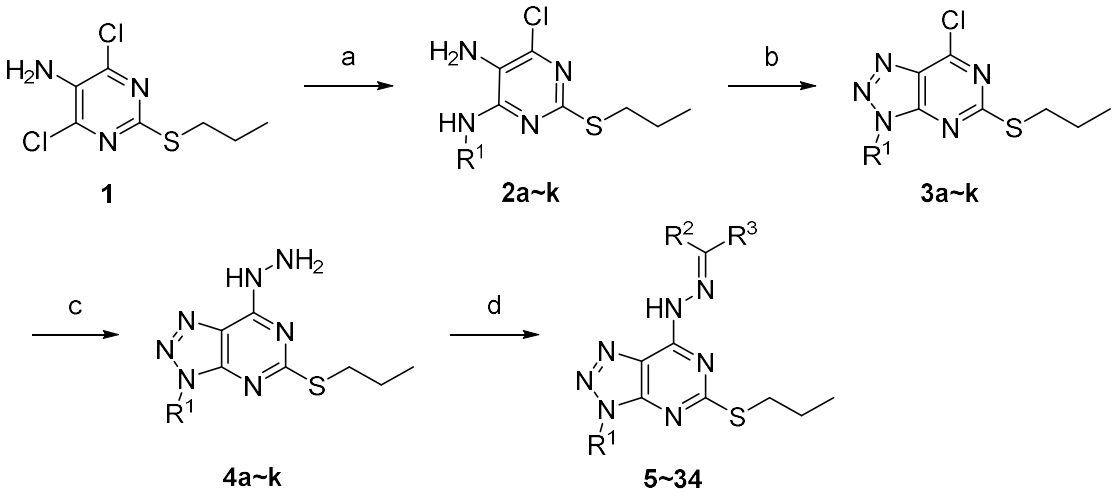

Scheme 1. Reagents and conditions: (a) appropriate amines, TEA, ethanol, 120 °C, 30 h, 50%~90%; (b) $NaNO_2$, AcOH, H_2O, 0~5 °C, 1~2 h, 51%~87%; (c) hydrazine hydrate, ethanol, rt, 4 h, 86%~95%; (d) appropriate aromatic aldehydes and ketones, ethanol, reflux, 4~8 h 71%~94%.

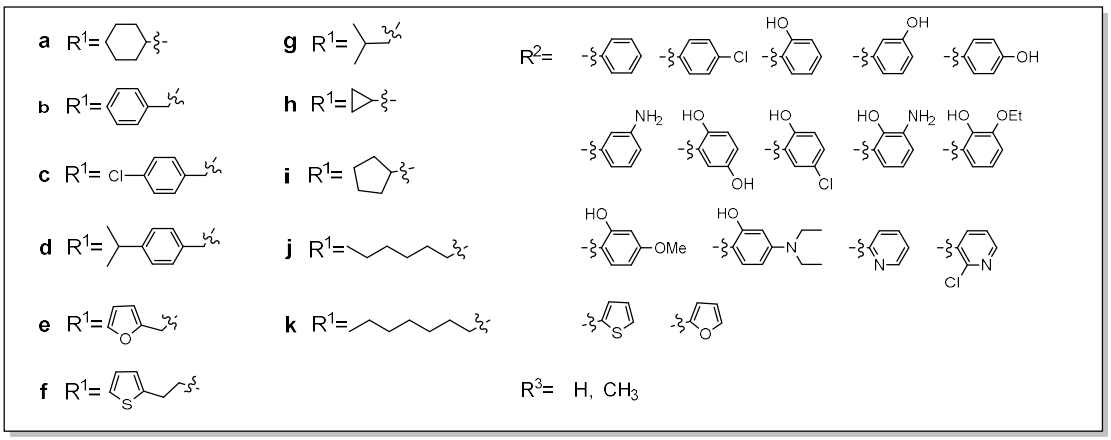

2.2 Evaluation of biological activity

2.2.1 Antiproliferative activity

Compounds **5~34** were evaluated for their antiproliferative activities against five cancer cell lines, including MGC-803 (human gastric cancer cell line), PC3 (human prostate cancer cell line), PC9 (human lung cancer cell line), EC9706 (human esophageal carcinoma cell line) and SMMC-7721 (human liver cancer cell line), using MTT assay. 5-fluorouracil (**5-FU**) was employed as a positive control. The preliminary data was summarized in Tables 1 and 2. Then we would analyze the structure activity relationship from PC3 cancer cell line.

Initially, fixing R^1 and R^2 as cyclohexyl and H, we introduced different hydrazine substituent to the scaffold. As shown in Table 1, comparing compound **5** with **6**, compound **6** with 4-chlorophenyl exhibited no cytotoxicity (IC_{50} > 50 nM). Then, we introduced the substituent of 2-OH which played a key role in improving activity against PC3 in previous work[27] and synthesized compounds **7~11**. But only **10** had little degree enhancement, and the selectivity showed no significant improvement. Next, we surprisingly found that compound **12** with pyridyl group displayed dramatically potent anticancer activity, especially on PC3 cells with IC_{50} value of 194.62 nM. However, after introducing an electron-withdrawing group, chloro-, to pyridyl group, compound **13** gave no cytotoxic activity (IC_{50} > 50 μM). Moreover, after replacing pyridyl with weaker aromatic furanyl or thienyl, compound **14** only kept a quite weak antiproliferative activity for PC3 and compound **15** totally lost the activity for all cancer cell lines. Hence, we inferred that the moderate aromaticity of R^3 like pyridyl maybe possessed more powerful inhibition.

Next, we replaced H on R^2 with CH_3 and synthesized compounds **16~24**. Comparing compounds **5** (H) and **7** (2-OH) with **16** (H) and **19** (2-OH), respectively, we found that compounds with H on R^2 exhibited a bit higher activity against PC3 than the compounds with H substituent. However, comparing compound **6** (4-Cl) with **18** (4-Cl), the activity against PC3 of compounds with CH_3 on R^2 showed a significant improvement, so we inferred that the choice which is more beneficial, between H and CH_3 on R^2 was determined by the performance of R^3. Furthermore, to explore the effect of position of benzene ring substituent on activity, we synthesized compounds **19**, **20** and **21** with ortho-, meta- and para-OH. The results showed that compound **20** with hydroxyl group positioned at meta- position lost the inhibitory activity, while compounds **19** and **21** still had cytotoxicity to some extent, but the selectivity between PC3 and other cell lines was very poor. A similar phenomenon was observed for compounds **17**, **22**, **23** and **24**, indicating that in this scaffold, the meta-H of benzene ring played a key role in the inhibition.

Table 1

Inhibitory results of compounds **5~24** against five cancer cell lines.

Comp.	R^1	R^2	R^3	$IC_{50}(\mu M)^a$				
				MGC-803	PC3	PC9	EC9706	SMMC-7721
5	cyclohexyl	H	Ph	14.10±1.14	1.21±0.08	4.61±0.66	7.42±0.87	9.67±0.98
6	cyclohexyl	H	4-Cl-Ph	>50	>50	>50	>50	>50
7	cyclohexyl	H	2-OH-Ph	11.86±1.07	3.63±0.35	3.70±0.56	13.36±1.12	7.85±0.89
8	cyclohexyl	H	2-OH-5-Cl -Ph	>50	>50	>50	>50	>50
9	cyclohexyl	H	2-OH-4- DEA-Ph	>50	>50	>50	>50	>50
10	cyclohexyl	H	2-OH-4-MeO-Ph	6.26±0.79	1.10±0.01	6.07±0.78	16.15±1.20	11.39±1.05
11	cyclohexyl	H	2-OH-3-EtO-Ph	>50	>50	>50	>50	>50
12	cyclohexyl	H		1.50±0.17	0.194±0.002	0.905±0.002	0.774 ±0.002	1.199±0.003
13	cyclohexyl	H		>50	>50	>50	>50	>50
14	cyclohexyl	H		24.22±1.38	2.90±0.46	11.54±1.06	8.01±0.90	8.93±0.95
15	cyclohexyl	H		>50	>50	>50	>50	>50
16	cyclohexyl	CH_3	Ph	34.63±2.17	1.57±0.31	3.43±0.56	11.86±1.07	15.90±1.20
17	cyclohexyl	CH_3	3-NH_2-Ph	>50	>50	>50	>50	>50
18	cyclohexyl	CH_3	4-Cl-Ph	12.84±1.10	0.78±0.10	3.60±0.55	9.82±0.99	20.13±1.30
19	cyclohexyl	CH_3	2-OH-Ph	4.40±0.64	5.23±0.37	3.25±0.51	3.96±0.59	8.89±0.94
20	cyclohexyl	CH_3	3-OH-Ph	>50	>50	>50	>50	>50
21	cyclohexyl	CH_3	4-OH-Ph	18.79±1.27	4.76±0.67	4.11±0.61	9.44±0.97	16.95±1.22
22	cyclohexyl	CH_3	2,5-diOH-Ph	>50	>50	>50	>50	>50
23	cyclohexyl	CH_3	2-OH-5-Cl -Ph	>50	>50	>50	>50	>50
24	cyclohexyl	CH_3	2-OH-3-NH_2-Ph	>50	>50	>50	>50	>50
5-Fu	—	—	—	8.14±0.80	6.89±0.65	7.26±0.71	5.76±0.62	11.25±1.05

[a] Inhibitory activity was assayed by exposure for 72 h to substance and expressed as concentration required to inhibit tumor cell proliferation by 50% (IC_{50}). Data are presented as the means ± SDs of three independent experiments (unit: μM/L).

To further explore the structure-activity relationship and obtain more selective and

powerful compounds, compounds **25~34** were synthesized. These compounds were designed based on the most potent compound **12** in Table 1, whose R^2 and R^3 were fixed as H and pyridyl, and R^1 was substituted with different groups. Their antiproliferative activities against five cancer cell lines were shown in Table 2. Comparing to compound **12**, replacement of cyclohexyl with benzyl (compound **25)** led to an obvious increase of the activity, and **25** also showed better selectivity between PC3 and other cancer cell lines. Furthermore, after adding a substituent to the benzyl ring, compound with an electron-withdrawing substituent, namely, **26** (IC_{50} = 71 nM), suggested better potency than **27** with an electron-donating substituent. This result indicated that electron-withdrawing group at the para-position of the benzyl may be more favorable for PC3 inhibitory activity than electron-donating group. While, if R^1 was furanmethyl (**28**) or 2-thienylethyl (**29**), the antiproliferative activity against PC3 was slightly decreased compared to **25**, and the selectivity for PC3 also declined. Additionally, when the aromatic ring was replaced with some aliphatic hydrocarbon, the results showed that isobutyl (**30**) and cyclopropyl (**31**) substituent, small volume groups, punily decreased the activity of PC3 and had bad selectivity between PC3 and PC9. However, compound **32** which bears a larger aliphatic cyclic hydrocarbon group (cyclopentyl), had higher activity for PC3 cells, but the selectivity still not so good. These results indicated that the volume of aliphatic hydrocarbon maybe affected the antitumor activity and selectivity. Moreover, R^1 were also replaced by long-chain alkanes. The anticancer activity of **33** and **34** with n-hexyl and n-heptyl replacement, respectively, were dramatically increased, especially compound **34** (IC_{50} = 26 nM) against PC3 cells, and as the carbon chain growing, the selectivity between PC3 and other cancer cell lines was also dramatically increased. This result suggested that the long-chain alkanes were excellently beneficial to the activity and selectivity. The detailed illustration for SAR studies of target derivatives against PC3 cell line was exhibited in Fig. 3.

These derivatives not only possessed good inhibition for five different cancer cell lines, most of them still displayed obvious selectivity for PC3 cell line compared to other four cell lines, especially compound **34** which had specially significant PC3 selectivity with index values of 21.42, 5.69, 153.46 and 32.46 for MGC-803, PC9, EC9706 and SMMC-7721 respectively. The selectivity index of all compounds between PC3 and MGC-803, PC9, EC9706 or SMMC-

7721 cell lines was also calculated as shown in Table 3. Hence, we chose compound **34** as optimal compound for further biological mechanisms.

Table 2

Inhibitory results of compounds **12** and **25~34** against five cancer cell lines.

Comp.	R^1	R^2	R^3	$IC_{50}(\mu M)^a$				
				MGC-803	PC3	PC9	EC9706	SMMC-7721
12	cyclohexyl	H		1.50±0.17	0.194±0.002	0.905±0.002	0.774±0.003	1.199±0.003
25	Bn	H		0.675±0.002	0.086±0.001	0.793±0.002	3.09±0.49	0.862±0.003
26	4-Cl-Bn	H		0.500±0.002	0.071±0.001	0.258±0.002	10.95±1.01	1.15±0.04
27	4-isopropyl-Bn	H		0.720±0.002	0.232±0.002	0.342±0.002	14.81±1.17	1.08±0.03
28	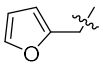	H		0.425±0.002	0.151±0.002	0.901±0.003	1.35±0.13	0.845±0.003
29	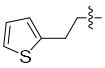	H		0.647±0.002	0.294±0.002	0.447±0.002	1.62±0.21	0.345±0.002
30	isobutyl	H		1.00±0.01	0.194±0.002	0.189±0.002	2.67±0.42	0.698±0.002
31	cyclopropyl	H		1.23±0.09	0.332±0.002	0.189±0.002	1.57±0.19	0.977±0.003
32	cyclopentyl	H		0.185±0.002	0.167±0.002	0.503±0.002	1.39±0.14	0.476±0.002
33	n-hexyl	H		0.855±0.003	0.097±0.002	0.270±0.002	0.903±0.003	0.440±0.002
34	n-heptyl	H		0.557±0.002	0.026±0.001	0.148±0.002	3.99±0.60	0.844±0.003
5-Fu	—	—	—	8.14±0.80	6.89±0.65	7.26±0.71	5.76±0.62	11.25±1.05

[a] Inhibitory activity was assayed by exposure for 72 h to substance and expressed as concentration required to inhibit tumor cell proliferation by 50% (IC_{50}). Data are presented as the means ± SDs of three independent experiments (unit: μM/L).

Table 3

The selectivity index of all compounds between PC3 and MGC-803, PC9, EC9706 or SMMC-7721 cell lines.

Comp.	R^1	R^2	R^3	Selectivity index

				SI_1[a]	SI_2[b]	SI_3[c]	SI_4[d]
5	cyclohexyl	H	Ph	11.65	3.81	6.13	7.99
6	cyclohexyl	H	4-Cl-Ph	1	1	1	1
7	cyclohexyl	H	2-OH-Ph	3.27	1.02	3.68	2.16
8	cyclohexyl	H	2-OH-5-Cl -Ph	1	1	1	1
9	cyclohexyl	H	2-OH-4- DEA-Ph	1	1	1	1
10	cyclohexyl	H	2-OH-4-MeO-Ph	5.69	5.52	14.68	10.35
11	cyclohexyl	H	2-OH-3-EtO-Ph	1	1	1	1
12	cyclohexyl	H		7.73	4.66	3.99	6.18
13	cyclohexyl	H		1	1	1	1
14	cyclohexyl	H		8.35	3.98	2.76	3.08
15	cyclohexyl	H		1	1	1	1
16	cyclohexyl	CH_3	Ph	22.06	2.18	7.55	10.13
17	cyclohexyl	CH_3	3-NH_3-Ph	1	1	1	1
18	cyclohexyl	CH_3	4-Cl-Ph	16.46	4.62	12.59	25.81
19	cyclohexyl	CH_3	2-OH-Ph	0.84	0.62	0.76	1.70
20	cyclohexyl	CH_3	3-OH-Ph	1	1	1	1
21	cyclohexyl	CH_3	4-OH-Ph	3.95	0.86	1.98	3.56
22	cyclohexyl	CH_3	2,5-diOH-Ph	1	1	1	1
23	cyclohexyl	CH_3	2-OH-5-Cl -Ph	1	1	1	1
24	cyclohexyl	CH_3	2-OH-3-NH_3-Ph	1	1	1	1
25	Bn	H		7.85	9.22	35.93	10.02
26	4-Cl-Bn	H		7.04	3.63	154.23	16.20
27	4-isopropyl-Bn	H		3.10	1.47	63.84	4.66

28	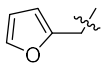	H		2.81	5.97	8.94	5.60
29	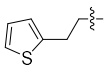	H		2.20	1.52	5.51	1.17
30	isobutyl	H		5.15	0.97	13.76	3.60
31	cyclopropyl	H		3.70	0.57	4.73	2.94
32	cyclopentyl	H		1.11	3.01	8.32	2.85
33	n-hexyl	H		8.81	2.78	9.31	4.54
34	n-heptyl	H		21.42	5.69	153.46	32.46
5-Fu	—	—	—	1.18	1.05	0.84	1.63

[a] The selectivity index (SI_1) was calculated as IC_{50} (MGC-803)/IC_{50} (PC3)

[b] The selectivity index (SI_2) was calculated as IC_{50} (PC9)/IC_{50} (PC3)

[c] The selectivity index (SI_3) was calculated as IC_{50} (EC9706)/IC_{50} (PC3)

[d] The selectivity index (SI_4) was calculated as IC_{50} (SMMC-7721)/IC_{50} (PC3)

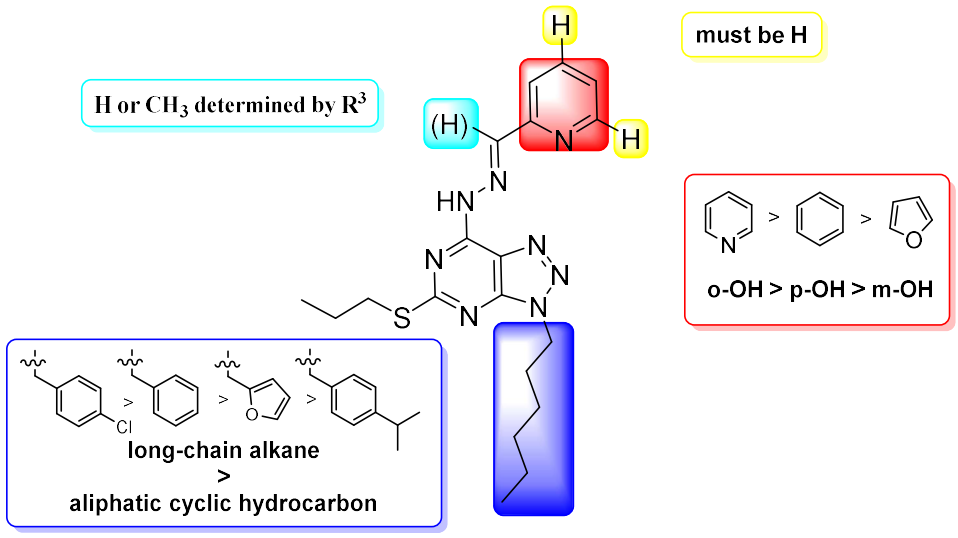

Fig. 3. SARs summary for the compounds against PC3 cell line.

*2.2.2. Compound **34** suppressed the proliferation of several cancer cell lines*

Based on the antiproliferative activity results of all compounds (Tables 1 and 2) and selectivity index results (Table 3), the most potent and selective **34** was prioritized to perform further experiments for evaluating antiproliferative mechanisms. We investigated the cytotoxicity of compound **34** on three normal cell lines (Het-1A, L02 and GES-1) by MTT assay for 72 h. The results showed that compound **34** had high selectivity for PC3 cells rather

than normal cells (Fig. 4C). Furthermore, except for PC3 cells, PC9 cells were selected as well for the following biological evaluations of compound **34**. We found that **34** inhibited the cell viabilities of PC3 and PC9 cells in a time- and dose-dependent manner (Fig. 4A, 4B and 4D). Colony formation assay also presented that **34** treated cells formed much fewer and smaller colonies, compared those with DMSO-treated cells (Fig. 4E and 4F). All these results suggested that **34** had a remarkable antiproliferative activity for PC3 cells.

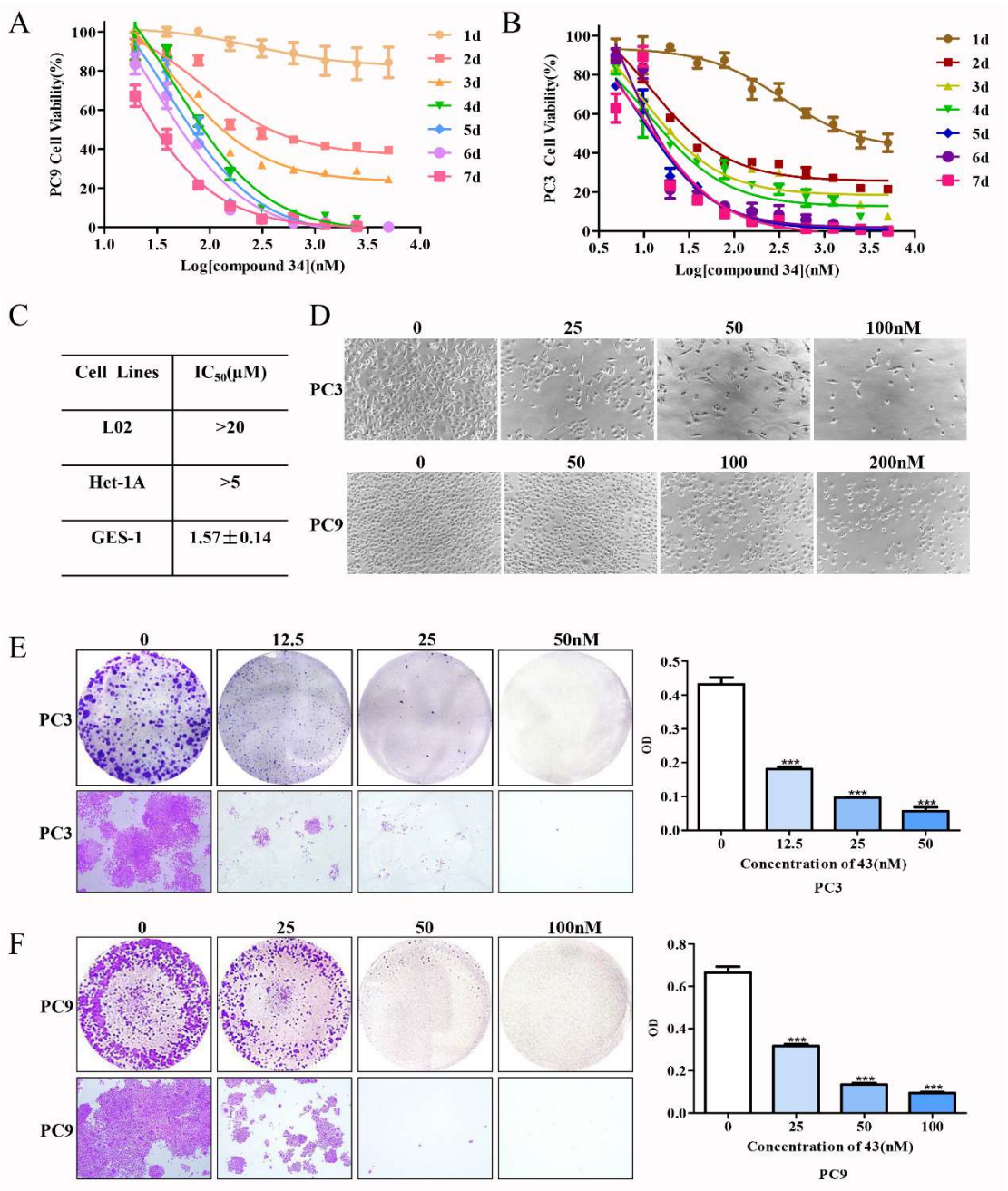

Fig. 4 Compound **34** inhibited the proliferation of PC3 and PC9 cells. (A and B) PC3 and PC9

cells were treated with serial dilutions of **34** for 1~7 days, then their viabilities were determined by MTT assay. (C) The cell viabilities of L02, Het-1A and GES-1 were measured after being incubated with **34** for 72 h. (D) Cells were treated with (0, 25, 50, 100 nM for PC3 or 0, 50, 100, 200 nM for PC9) **34** for 72 h and captured by microscope (magnification: 100×). PC3 (E) and PC9 (F) cells clonogenicity assays were performed and quantified after 0, 12.5, 25, 50 nM or 0, 25, 50, 100 nM **34** treatment for 7 days. Three individual experiments were performed for each group. The data were expressed as the Mean ± SD. The symbols *, ** or *** stand for $P<0.05$, $P<0.01$ or $P<0.001$ compared with the controls.

*2.2.3. Compound **34** induced ROS production*

Furthermore, we all know that reactive oxygen species (ROS) act as a double-edged sword in living cells [32]. On one hand, it plays essential roles in maintaining vital biological functions [33]. On the other hand, excessive ROS inhibits the growth of cancer cells [34, 35]. To explore whether the remarkable anti-proliferative activity of **34** is related to ROS level, we measured the intracellular ROS level after PC3 and PC9 cells being treated with **34** for 72 h, using the reactive oxygen assay kit. The results showed that **34** treatments significantly increased their intracellular ROS content (Fig. 5A, 5C and 5D). Moreover, like previous findings [36], the elevating intracellular ROS level activated MAPK signaling pathway and further increased the phosphorylation level of its downstream proteins: P38 and JNK (Fig. 5B, 5E and 5F). After adding an antioxidant NAC (N-acetyl-Lcysteine, 5 mM) to PC3 cells, the phenomena were revised to some extent: the survival rates in cells were increased, the expression levels of p-P38, p-JNK and apoptosis-related proteins (Bax and cleaved-Caspased 3) were decreased and the expression level of anti-apoptotic protein (Bcl-2) was increased, compared those with only **34** treatment cells (Fig. 5G-5I). These results suggested that the remarkably raised ROS level indeed played a crucial role in the survival of these cancer cells.

Peroxiredoxins (Prx I-VI) are a family of antioxidants that protect cells from metabolically produced reactive oxygen species. They are found in a wide variety of species and exert an enormous function on peroxide detoxification [29, 36]. Therefore, the expression levels of Prx I-VI were measured in PC3 and PC9 cells after **34** treatment (Fig. 5J-5L). The results exhibited

that the expression levels of Prx I-III were obviously increased, while there was no change for Prx IV-VI. Based on these results, we speculated that the reason was the highly raised ROS level, which reversely stimulated Prx I-III expression in order to eliminate them, but more exact and detailed mechanisms need further profound exploration.

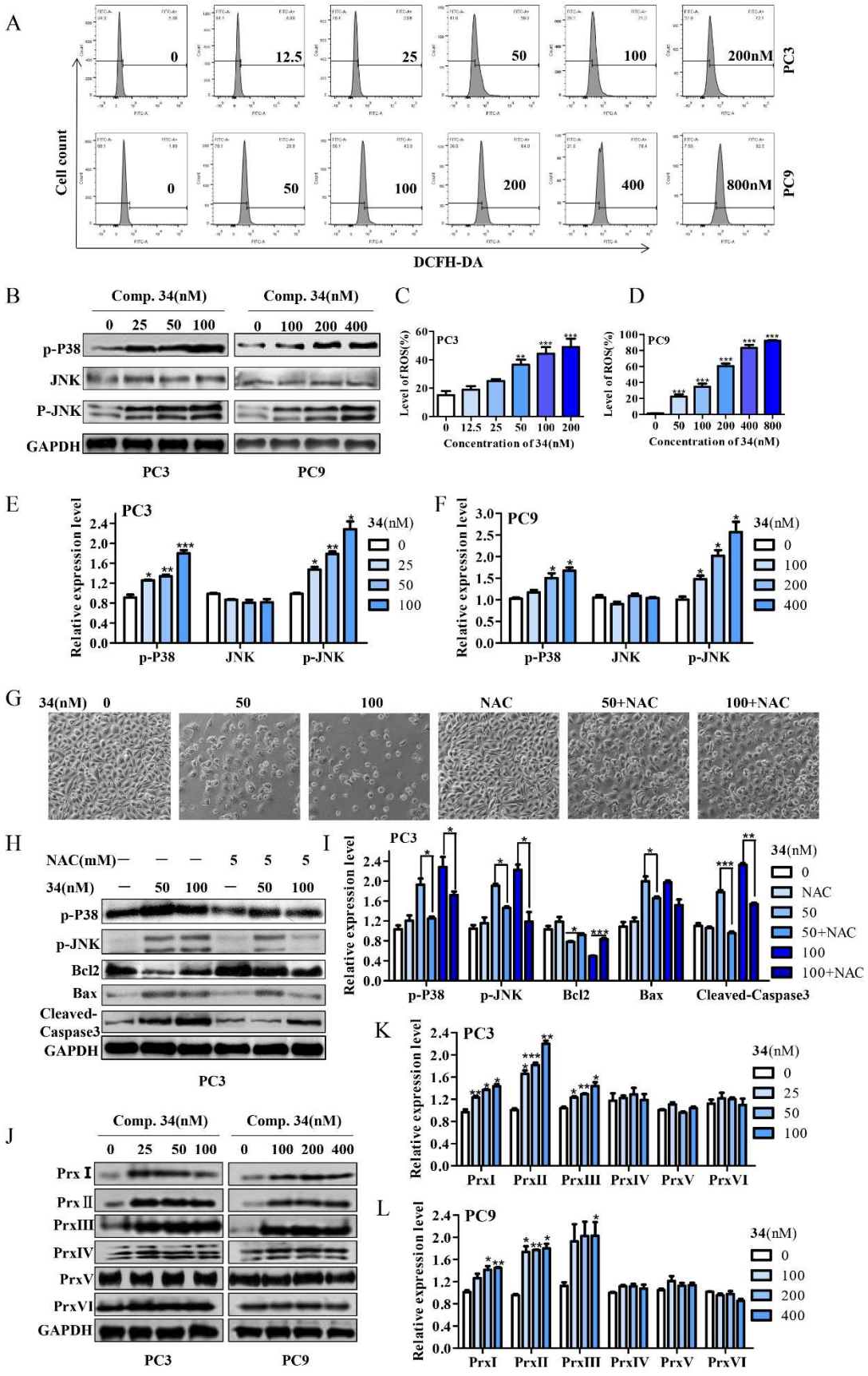

Fig. 5 Compound **34** induced ROS production. (A) PC3 and PC9 cells were treated with **34** for 72 h (0, 12.5, 25, 50, 100, 200 nM for PC3, 0, 50, 100, 200, 400, 800 nM for PC9) and thereafter

loaded with 10 mM DCFH-DA for the examination of ROS. The levels of ROS in PC3 (C) and PC9 (D) cells were quantified by flow cytometry. (B) Western Blot analysis of the protein levels of p-P38, JNK and p-JNK in PC3 and PC9 cells, treated with increasing concentrations (0, 25, 50, 100 nM for PC3; 0, 100, 200, 400 nM for PC9) of **34**. (E and F) Densitometry shows relative protein expression normalized for GAPDH. PC3 cells were pretreated with NAC (5 mM) for 1 h, followed with **34**. (G) The cells were captured by the microscope (magnification: 100×). The protein levels of p-P38, p-JNK, Bcl-2, Bax and Cleaved-Caspase 3 were determined by Western Blot (H) and quantified by Image J software (I). After **34** treatment, the Prx I-VI expression levels in PC3 and PC9 cells were measured by Western Blot (J) and quantified by Image J software (K and L). Three individual experiments were performed for each group. The symbols *, ** or *** stand for $P<0.05$, $P<0.01$ or $P<0.001$ compared with the controls.

*2.2.4. Compound **34** suppressed EGFR expression*

It is well-known that ERK is one part of MAPK pathway, while we surprisingly found that **34** obviously decreased the phosphorylation level of ERK rather than increased it (Fig. 6C, 6E and 6F). **34** could greatly inhibit PC3 and PC9 which is known as EGFR-expressing human prostate and lung cancer cell lines. Moreover, the structure of **34** contains anilinopyrimidine, one of EGFR symbolic skeleton [37, 38], so we infer that **34** may have a certain inhibitory effect on EGFR. To make it clear, we determined the expression level of epidermal growth factor receptor (EGFR) after **34** treatments. We found that **34** obviously decreased the mRNA (Fig. 6B) and protein levels of EGFR in a dose-dependent manner (Fig. 6A and 6D). Moreover, the phosphorylation level of AKT (Fig. 6C, 6E and 6F), another downstream signaling protein of EGFR [39], were significantly declined. Furthermore, previous work found that triazolopyrimidine derivatives were capable of inhibiting LSD1[26]. Therefore, we also tested **34** inhibition for LSD1, but the result showed no inhibitory activity. These results suggested that compound **34** could inhibit EGFR and restrain its downstream proteins: p-ERK and p-AKT.

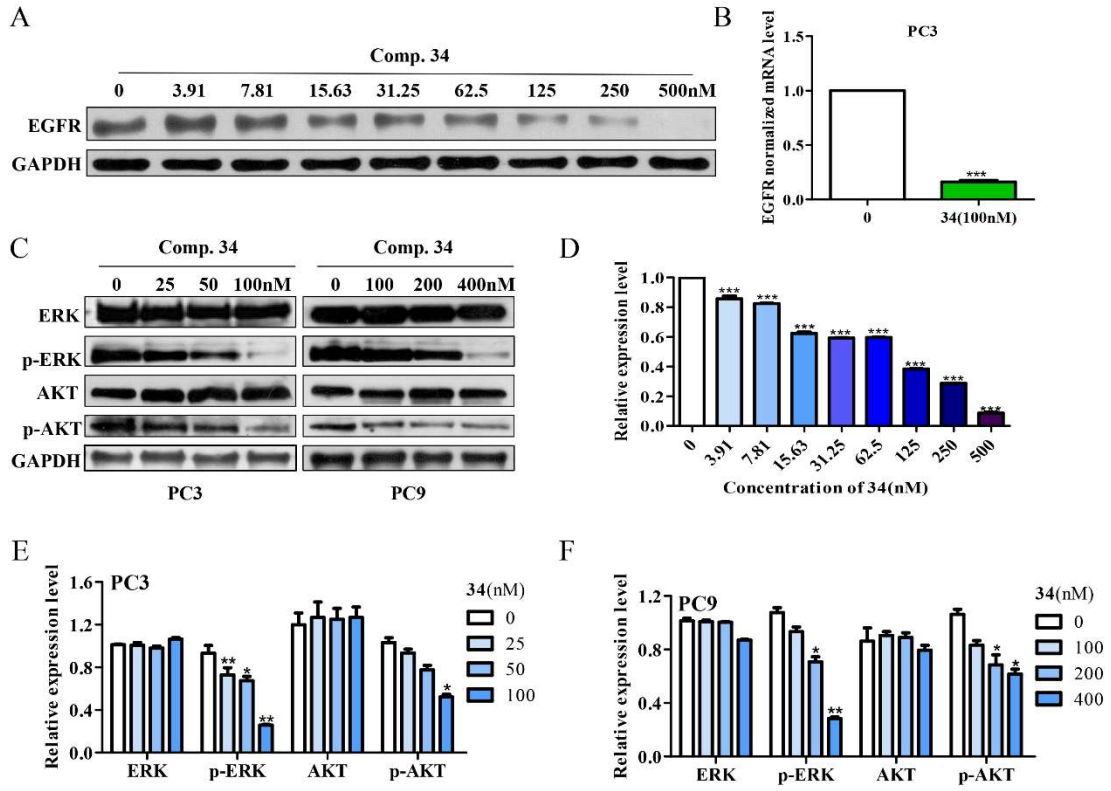

Fig. 6 Compound **34** decreased EGFR expression. (A) PC3 cells were treated with increasing concentrations (0~500 nM) of **34** for 72 h, the expression levels of EGFR were determined by Western Blot and quantified by Image J software (D). (B) After being treated with 100 nM **34** for 72 h, PC3 cells were collected for RNA-seq experiment. (C) Western Blot analysis of the protein levels of ERK, p-ERK, AKT and p-AKT in PC3 and PC9 cells, treated with increasing concentrations (0, 25, 50, 100 nM for PC3; 0, 100, 200, 400 nM for PC9) of **34**. (E and F) Densitometry shows relative protein expression normalized for GAPDH. Three individual experiments were performed for each group. The symbols *, ** or *** stand for $P<0.05$, $P<0.01$ or $P<0.001$ compared with the controls.

*2.2.5. Compound **34** induced PC3 and PC9 cells apoptosis*

Given that **34** potently inhibited the growth of PC3 and PC9 cells, induced ROS production, and decreased EGFR expression, we hypothesized that **34** should be capable of inducing apoptosis. As shown in Figure 7A, PC3 and PC9 cells, which were treated with **34** for 72 h, exhibited significant apoptosis-related morphologies, such as cell shrinkage, nuclear fragmentation and condensation, in a dose-dependent manner. Annexin V-FITC/PI double

staining also showed that **34** obviously increased the percentage of cell apoptosis dose-dependently (Fig. 7B-7E).

Moreover, a series of pro- and anti-apoptotic proteins were examined by Western Blot. As shown in Figure 7F-7H, **34** evidently increased the expression levels of Bax and P53 and significantly reduced the expression level of anti-apoptotic protein: Bcl-2. Furthermore, the cleaved caspase-8/9/3, cleaved PARP and cleaved BID (t-BID) were obviously increased dose-dependently. All these results indicated that **34** could remarkably induce PC3 and PC9 cells apoptosis. On the other hand, the concentration difference of **34** used for PC3 and PC9 cells further confirmed that **34** had excellent selectivity for PC3 cells.

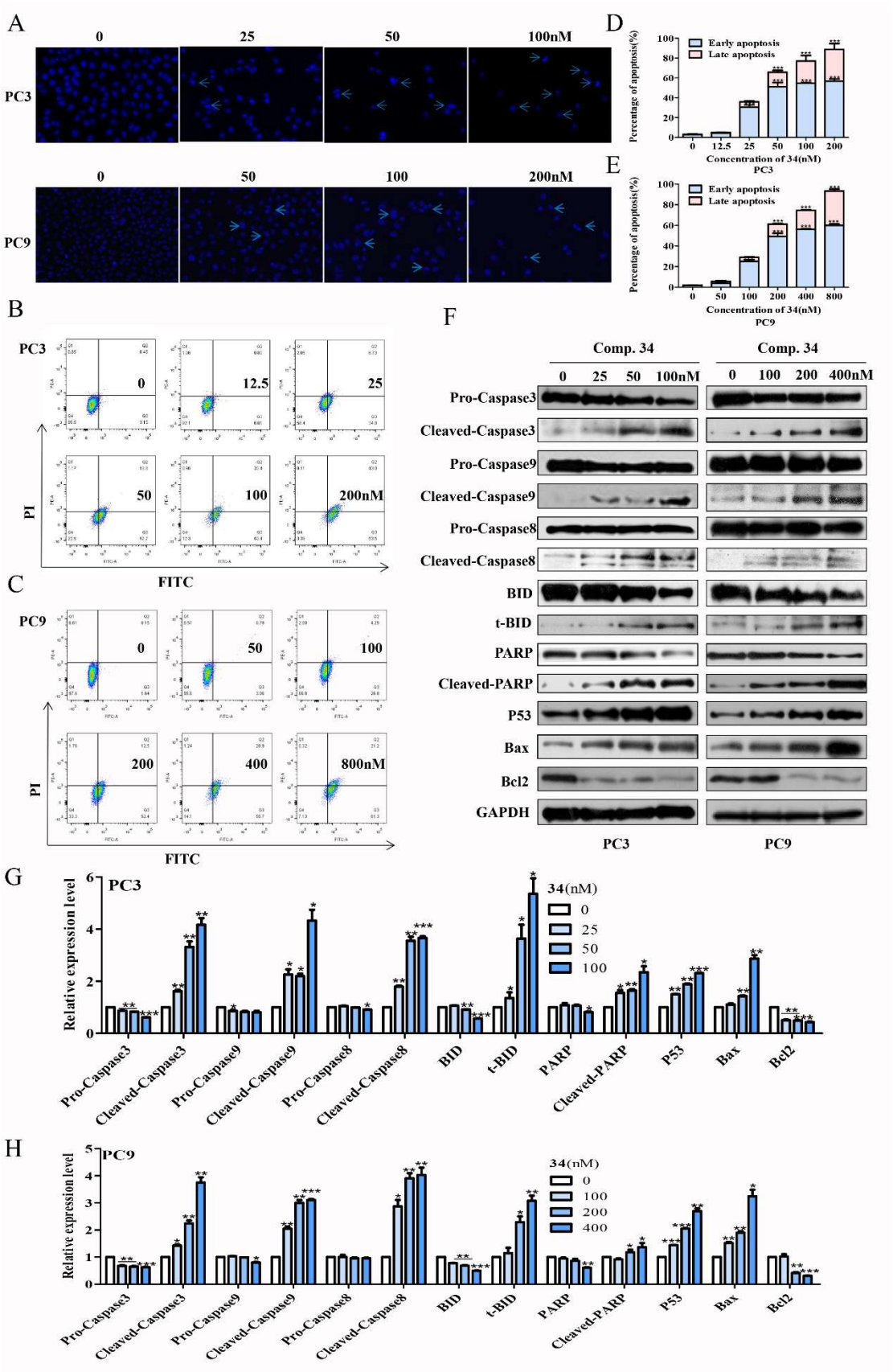

Fig. 7 Compound **34** induced apoptosis of PC3 and PC9 cells. (A) After being treated with **34** for 72 h (0, 25, 50, 100 nM for PC3; 0, 50, 100, 200 nM for PC9), PC3 and PC9 cells were

stained with Hoechst 33342 (marked with white arrows, magnification: 100×). (B-E) Quantitative analysis of apoptotic cells using Annexin V-FITC/PI double staining and flow-cytometry calculation (0, 12.5, 25, 50, 100, 200 nM for PC3; 0, 50, 100, 200, 400, 800 nM for PC9). (F) PC3 cells were treated with 0, 25, 50 and 100 nM or PC9 cells were treated with 0, 100, 200 and 400 nM **34** for 72 h and subjected to Western Blot analysis. (G and H) Quantitative analysis of the protein level. Three individual experiments were performed for each group. The symbols *, ** or *** stand for $P<0.05$, $P<0.01$ or $P<0.001$, compared with the controls.

3. Conclusion

In summary, a series of novel [1,2,3]triazolo[4,5-d]pyrimidine derivatives bearing hydrazone moiety was designed, synthesized and evaluated. Most compounds exhibited strong antiproliferative activities against five cancer cell lines (MGC-803, PC3, PC9, EC9706, SMMC-7721), and displayed obvious selectivity for PC3 cells compared to other cancer cell lines, especially compound **34**, which had the highest inhibitory effects on PC3 cancer cells, best selectivity between PC3 and the other cell lines and less toxicity on normal cells (L02, Het-1A and GES-1). Further studies indicate that **34** has the ability to inhibit cancer cells colony formation, increase cellular ROS content, and induce cell apoptosis. The concentrations of compound **34** that were used for PC3 and PC9 cells further confirm that compound **34** possesses great selectivity for PC3. We also identified that **34** presented excellent inhibition of EGFR expression level. Consequently, our work suggests that [1,2,3]triazolo[4,5-d]pyrimidine derivatives bearing hydrazone scaffold is an excellent anticancer chemical skeleton against prostate cancer cell (PC3) and could be potentially utilized for designing more powerful antiproliferative agents. Compound **34** could be served as a starting point for further development of anti-prostatic cancer drug with improved potency and selectivity.

4. Experimental section

4.1 General

Reagents and solvents were purchased from commercial sources and were used without further purification. The reaction process was monitored by TLC (Thin Layer chromatography)

with silica gel plates (thickness 250 μm, Indicator F-254). The target analogs were purified by column chromatography with silica gel (300–400 meshes). Melting points were determined on an X-5 micromelting apparatus and were uncorrected. ^{1}H NMR and ^{13}C NMR spectra were recorded on a Bruker 400 MHz and 100 MHz spectrometers respectively. High-resolution mass spectra (HRMS) were recorded on a Waters Micromass Q-T of Micromass spectrometer by electrospray ionization (ESI)

4.2 General procedure for the synthesis of compounds 2a~k

The 4,6-dichloro-2-(propylthio)pyrimidin-5-amine **1** (1.00 eq), appropriate amine (1.05 eq) and triethylamine (3.00 eq) in ethanol were heated to 120 °C for 30 h. After completion, the residue was concentrated under vacuum and then diluted with water. After being adjusted to pH at 7 with 5% HCl, the mixture was extracted with ethyl acetate and washed with brine. Then, it was dried over $MgSO_4$. After removal of the solvent, the resulting residue was purified by column chromatography (PE/EA = 3:1~1:1) to acquire the pure compounds **2a~k**.

*4.2.1 6-chloro-N^4-cyclohexyl-2-(propylthio)pyrimidine-4,5-diamine (**2a**)*

Yellow solid, yield: 90%. ^{1}H NMR (400 MHz, DMSO-d_6) δ 6.66 (d, J = 6.9 Hz, 1H, NH), 4.80 (s, 2H, NH_2), 3.84 (d, J = 6.2 Hz, 1H, N-CH), 2.93 (t, J = 7.3 Hz, 2H, S-CH_2), 1.93 (d, J = 11.2 Hz, 2H, cyclohexyl CH_2), 1.75 (d, J = 12.0 Hz, 2H, CH_2), 1.67–1.61 (m, 3H, cyclohexyl CH_2), 1.41–1.10 (m, 5H, cyclohexyl CH_2), 0.96 (t, J = 7.3 Hz, 3H, CH_3). LC-MS (ESI): Calcd. $C_{13}H_{21}ClN_4S$, $[M+H]^+$m/z: 301.12, found: 301.14.

4.3 General procedure for the synthesis of compounds 3a~k

Compounds **2a~k** (1.00 eq) were dissolved in acetic acid and the mixture was cooled in an ice bath. Sodium nitrite (1.00 eq in small amount of water) was added to keep the reaction temperature below 5 °C. The resulting reaction mixture was stirred for 1~2 h at 0~5 °C. After completion, monitored by TLC (PE/EA = 1:1~1:3), the solution was diluted with double volume of ethyl acetate and washed with water for 3 times. Then, they were neutralized with saturated sodium bicarbonate. The organic layer was washed with brine and then dried over anhydrous sodium sulfate. The organic layer was concentrated under reduced pressure to give

the crude product which was used to the next step without further purification. Small amount of the crude product was purified by flash column chromatography for structure identification.

*4.3.1 7-chloro-3-cyclohexyl-5-(propylthio)-3H-[1,2,3]triazolo[4,5-d]pyrimidine (**3a**)*

Yellow solid, yield: 83%. ^{1}H NMR (400 MHz, DMSO-d_6) δ 4.90–4.59 (m, 1H, cyclohexyl CH), 3.22–3.15 (m, 2H, S-CH_2), 2.12 (d, J = 10.0 Hz, 2H, N-CH_2), 2.05 (t, J = 9.5 Hz, 2H, cyclohexyl CH_2), 1.89–1.86 (m, 2H, cyclohexyl CH_2), 1.79–1.74 (m, 3H, cyclohexyl CH_2), 1.57–1.51 (m, 2H, CH_2), 1.38–1.20 (m, 1H, cyclohexyl CH_2), 1.06–0.98 (m, 3H, CH_3). LC-MS (ESI): Calcd. $C_{13}H_{18}ClN_5S$, $[M+H]^+$m/z: 312.10, found: 312.19.

4.4 General procedure for the synthesis of compounds 4a~k

A mixture of **3a~k** (1.00 eq) in ethanol hydrazine hydrate (3.00 eq) was added. Then, the reaction was stirred at room temperature for 4 h, whose progress was monitored by TLC (PE/EA = 3:1~1:1) until it was completed. A crude solid was obtained by rotating evaporated solvent. The product was purified by recrystallization from ethanol.

*4.4.1 3-cyclohexyl-7-hydrazinyl-5-(propylthio)-3H-[1,2,3]triazolo[4,5-d]pyrimidine (**4a**)*

White solid, yield: 94%. ^{1}H NMR (400 MHz, DMSO-d_6) δ 10.15 (s, 1H, NH), 4.79 (s, 2H, NH_2), 4.64 (s, 1H, N-CH), 3.11 (t, J = 6.6 Hz, 2H, S-CH_2), 2.05 (s, 4H, cyclohexyl CH_2), 1.87 (d, J = 12.8 Hz, 2H, cyclohexyl CH_2), 1.80–1.65 (m, 3H, cyclohexyl CH_2), 1.47 (d, J = 6.9 Hz, 2H, CH_2), 1.31–1.25 (m, 1H, cyclohexyl CH_2), 1.00 (t, J = 7.1 Hz, 3H, CH_3). LC-MS (ESI): Calcd. $C_{13}H_{21}N_7S$, $[M+H]^+$m/z: 308.16, found: 308.26.

*4.4.2 3-benzyl-7-hydrazinyl-5-(propylthio)-3H-[1,2,3]triazolo[4,5-d]pyrimidine (**4b**)*

Yellow solid, yield: 91%. ^{1}H NMR (400 MHz, $CDCl_3$) δ 7.94 (s, 1H, NH), 7.46–7.40 (m, 2H, ArH), 7.37–7.29 (m, 3H, ArH), 5.68 (s, 2H, N-CH_2), 5.48 (bs, 2H, NH_2) 3.16 (t, J = 7.3 Hz, 2H, S-CH_2), 1.82–1.75 (m, 2H, CH_2), 1.07 (t, J = 7.4 Hz, 3H, CH_3). LC-MS (ESI): Calcd. $C_{14}H_{17}N_7S$, $[M+H]^+$m/z: 316.13, found: 316.21.

*4.4.3 3-(4-chlorobenzyl)-7-hydrazinyl-5-(propylthio)-3H-[1,2,3]triazolo[4,5-d]pyrimidine (**4c**)*

Brown solid, yield: 92%.^{1}H NMR (400 MHz, DMSO-d_6) δ 7.45–7.39 (m, 2H, ArH), 7.36–7.33 (m, 2H, ArH), 5.69 (s, 2H, N-CH_2), 5.04 (bs, 2H, NH_2) 3.10 (t, J = 7.0 Hz, 2H, S-CH_2), 1.72–1.60 (m, 2H, CH_2), 0.97 (t, J = 7.3 Hz, 3H, CH_3). LC-MS (ESI): Calcd. $C_{14}H_{16}ClN_7S$, $[M+H]^+$m/z: 350.09, found: 350.21.

4.4.4 7-hydrazinyl-3-(4-isopropylbenzyl)-5-(propylthio)-3H-[1,2,3]triazolo[4,5-d]pyrimidine ***(4d)***

Brown solid, yield: 93%. ^{1}H NMR (400 MHz, $CDCl_3$) δ 7.71 (s, 1H, NH), 7.38–7.35 (m, 2H, ArH), 7.20–7.16 (m, 2H, ArH), 5.64 (s, 2H, N-CH_2), 5.33 (bs, 2H, NH_2), 3.16 (t, J = 7.2 Hz, 2H, S-CH_2), 2.93–2.82 (m, 1H, CH), 1.82–1.76 (m, 2H, CH_2), 1.21 (d, J = 6.9 Hz, 6H, 2-CH_3), 1.07 (t, J = 7.4 Hz, 3H, CH_3). LC-MS (ESI): Calcd. $C_{17}H_{23}N_7S$, $[M+H]^+$m/z: 358.17, found: 358.29.

4.4.5 3-(furan-2-ylmethyl)-7-hydrazinyl-5-(propylthio)-3H-[1,2,3]triazolo[4,5-d]pyrimidine ***(4e)***

Pink solid, yield: 93%. ^{1}H NMR (400 MHz, DMSO-d_6) δ 7.62 (s, 1H, NH), 6.52 (d, J = 3.1 Hz, 1H, ArH), 6.47–6.42 (m, 1H, ArH), 5.69 (s, 2H, N-CH_2), 5.08 (bs, 2H, NH_2) 3.13 (t, J = 7.0 Hz, 2H, S-CH_2), 1.77–1.64 (m, 2H, CH_2), 1.00 (t, J = 7.3 Hz, 3H, CH_3). LC-MS (ESI): Calcd. $C_{12}H_{15}N_7OS$, $[M+H]^+$m/z: 306.11, found: 306.15.

4.4.6 7-hydrazinyl-5-(propylthio)-3-(2-(thiophen-2-yl)ethyl)-3H-[1,2,3]triazolo[4,5-d]pyrimidine ***(4f)***

Pink solid, yield: 95%. ^{1}H NMR (400 MHz, $CDCl_3$) δ 7.78 (s, 1H, NH), 7.14 (dd, J = 5.1, 1.1 Hz, 1H, ArH), 6.92–6.85 (m, 1H, ArH), 6.78 (d, J = 2.8 Hz, 1H, ArH), 6.33 (s, 2H, NH_2), 4.78 (t, J = 7.3 Hz, 2H, N-CH_2), 3.56 (t, J = 7.3 Hz, 2H, Ar-CH_2), 3.15 (t, J = 7.2 Hz, 2H, S-CH_2), 1.82–1.76 (m, 2H, CH_2), 1.07 (t, J = 7.4 Hz, 3H, CH_3). LC-MS (ESI): Calcd. $C_{13}H_{17}N_7S_2$, $[M+H]^+$m/z: 336.10, found: 336.18.

*4.4.7 7-hydrazinyl-3-isobutyl-5-(propylthio)-3H-[1,2,3]triazolo[4,5-d]pyrimidine (****4g****)*

Yellow solid, yield: 87%. ^{1}H NMR (400 MHz, DMSO-d_6) δ 4.97 (bs, 2H, NH_2) 4.28 (d, J = 7.0 Hz, 2H, N-CH_2), 3.12 (t, J = 7.0 Hz, 2H, S-CH_2), 2.33–2.24 (m, 1H, CH), 1.76–1.65 (m, 2H, CH_2), 0.99 (t, J = 7.3 Hz, 3H, CH_3), 0.88 (d, J = 6.7 Hz, 6H, 2-CH_3). LC-MS (ESI): Calcd. $C_{11}H_{19}N_7S$, $[M+H]^+$m/z: 282.14, found: 282.18.

*4.4.8 3-cyclopropyl-7-hydrazinyl-5-(propylthio)-3H-[1,2,3]triazolo[4,5-d]pyrimidine (**4h**)*

Brown solid, yield: 90%. ^{1}H NMR (400 MHz, $CDCl_3$) δ 7.83 (s, 1H, NH), 4.29 (bs, 2H, NH_2), 3.92–3.83 (m, 1H, N-CH), 3.18 (t, J = 7.2 Hz, 2H, S-CH_2), 1.85–1.78 (m, 2H, CH_2), 1.53–1.44 (m, 2H, cyclopropyl CH_2), 1.27–1.21 (m, 2H, cyclopropyl CH_2), 1.08 (t, J = 7.4 Hz, 3H, CH_3). LC-MS (ESI): Calcd. $C_{10}H_{15}N_7S$, $[M+H]^+$m/z: 266.11, found: 266.23.

*4.4.9 3-cyclopentyl-7-hydrazinyl-5-(propylthio)-3H-[1,2,3]triazolo[4,5-d]pyrimidine (**4i**)*

Orange solid, yield: 92%. ^{1}H NMR (400 MHz, $CDCl_3$) δ 6.70 (s, 1H, NH) 5.26–5.17 (m, 1H, N-CH), 4.24 (bs, 2H, NH_2) 3.16 (t, J = 7.2 Hz, 2H, S-CH_2), 2.32–2.20 (m, 4H, cyclopentyl CH_2), 2.08–1.98 (m, 2H, CH_2), 1.84–1.75 (m, 4H, cyclopentyl CH_2), 1.07 (t, J = 7.4 Hz, 3H, CH_3). LC-MS (ESI): Calcd. $C_{12}H_{19}N_7S$, $[M+H]^+$m/z: 294.14, found: 294.19.

*4.4.10 3-hexyl-7-hydrazinyl-5-(propylthio)-3H-[1,2,3]triazolo[4,5-d]pyrimidine (**4j**)*

Brown solid, yield: 88%. ^{1}H NMR (400 MHz, DMSO-d_6) δ 4.98 (bs, 2H, NH_2) 4.45 (t, J = 6.9 Hz, 2H, N-CH_2), 3.12 (t, J = 7.0 Hz, 2H, S-CH_2), 1.95–1.84 (m, 2H, CH_2), 1.77–1.66 (m, 2H, CH_2), 1.31–1.17 (m, 6H, CH_2), 0.99 (t, J = 7.3 Hz, 3H, CH_3), 0.82 (t, J = 6.7 Hz, 3H, CH_3). LC-MS (ESI): Calcd. $C_{13}H_{23}N_7S$, $[M+H]^+$m/z: 310.17, found: 310.23.

*4.4.11 3-heptyl-7-hydrazinyl-5-(propylthio)-3H-[1,2,3]triazolo[4,5-d]pyrimidine (**4k**)*

Brown solid, yield: 86%. ^{1}H NMR (400 MHz, DMSO-d_6) δ 4.78(bs, 2H, NH_2) 4.44 (t, J = 6.8 Hz, 2H, N-CH_2), 3.12 (t, J = 7.1 Hz, 2H, S-CH_2), 1.94–1.84 (m, 2H, CH_2), 1.77–1.65 (m, 2H, CH_2), 1.32–1.15 (m, 8H, CH_2), 0.99 (t, J = 7.3 Hz, 3H, CH_3), 0.83 (t, J = 6.8 Hz, 3H, CH_3). LC-MS (ESI): Calcd. $C_{14}H_{25}N_7S$, $[M+H]^+$m/z: 324.19, found: 324.22.

4.5 General procedure for the synthesis of compounds 5~34

Appropriate aromatic aldehyde or ketone (1.50 eq) and compounds **4a~k** (1.00 eq) were dissolved in ethanol. Then, the reaction mixture was refluxed for 4~8 h. After cooling, the solvents were removed and the crude product was purified by column chromatography using methanol/dichloromethane = 1%~5% as eluent to give final compounds **5~34.**

*4.5.1 7-(2-benzylidenehydrazinyl)-3-cyclohexyl-5-(propylthio)-3H-[1,2,3]triazolo[4,5-d]pyrimidine (**5**)*

Yellow solid, yield: 74%; m.p.: 124–126 °C. IR (KBr) cm^{-1}, 3203 (NH), 3041 (CH-Ar), 2960 (CH), 2931 (CH), 2859 (CH), 1571 (C=N). ^1H NMR (400 MHz, $CDCl_3$) δ 9.53 (s, 1H, NH), 8.09 (s, 1H, N=CH), 7.89–7.81 (m, 2H, ArH), 7.44–7.41 (m, 3H, ArH), 4.77–4.72 (m, 1H, N-CH), 3.19 (t, *J* = 7.2 Hz, 2H, S-CH_2), 2.22–2.13 (m, 4H, cyclohexyl CH_2), 1.98 (d, *J* = 13.5 Hz, 2H, cyclohexyl CH_2), 1.86–1.78 (m, 3H, cyclohexyl CH_2), 1.53–1.47 (m, 2H, CH_2), 1.42–1.33 (m, 1H, cyclohexyl CH_2), 1.08 (t, *J* = 7.4 Hz, 3H, CH_3). ^{13}C NMR (100 MHz, $CDCl_3$) δ 133.7, 130.4, 128.8, 127.7, 57.8, 33.4, 32.1, 25.5, 25.3, 22.8, 13.6. HR-MS (ESI): Calcd. $C_{20}H_{25}N_7S$, $[M+Na]^+$m/z: 418.1784, found: 418.1789.

*4.5.2 7-(2-(4-chlorobenzylidene)hydrazinyl)-3-cyclohexyl-5-(propylthio)-3H-[1,2,3]triazolo[4,5-d]pyrimidine (**6**)*

White solid, yield: 77%; m.p.: 186–189 °C. IR (KBr) cm^{-1}, 3159 (NH), 3049 (CH-Ar), 2963 (CH), 2935 (CH), 2864 (CH), 1575 (C=N). ^1H NMR (400 MHz, DMSO-d_6) δ 12.47 (s, 1H, NH), 8.26 (s, 1H, N=CH), 7.88–7.75 (m, 2H, ArH), 7.58–7.52 (m, 2H, ArH), 4.77–4.65 (m, 1H, N-CH), 3.14 (t, *J* = 7.2 Hz, 2H, S-CH_2), 2.16–2.02 (m, 4H, cyclohexyl CH_2), 1.89 (d, *J* = 13.3 Hz, 2H, cyclohexyl CH_2), 1.81–1.68 (m, 3H, cyclohexyl CH_2), 1.57–1.44 (m, 2H, CH_2), 1.34–1.20 (m, 1H, cyclohexyl CH_2), 1.03 (t, *J* = 7.3 Hz, 3H, CH_3). ^{13}C NMR (100 MHz, DMSO-d_6) δ 154.1, 131.0, 127.0, 123.8, 123.5, 52.6, 28.1, 26.9, 20.2, 20.0, 17.6, 8.4. HR-MS (ESI): Calcd. $C_{20}H_{24}ClN_7S$, $[M+H]^+$m/z: 430.1575, found: 430.1581.

*4.5.3 2-((2-(3-cyclohexyl-5-(propylthio)-3H-[1,2,3]triazolo[4,5-d]pyrimidin-7-yl)hydrazono)methyl)phenol (**7**)*

White solid, yield: 80%; m.p.: 194–196 °C. IR (KBr) cm^{-1}, 3362 (OH), 3215 (NH), 3045

(CH-Ar), 2926 (CH), 2854 (CH), 1580 (C=N). ^{1}H NMR (400 MHz, $CDCl_3$) δ 11.16 (s, 1H, OH), 10.87 (s, 1H, NH), 8.33 (s, 1H, N=CH), 7.28 (dd, *J* = 7.2, 5.5 Hz, 1H, ArH), 7.15 (d, *J* = 6.6 Hz, 1H, ArH), 7.06 (d, *J* = 8.2 Hz, 1H, ArH), 6.84 (t, *J* = 6.7 Hz, 1H, ArH), 4.72 (m, 1H, N-CH), 2.96 (t, *J* = 7.3 Hz, 2H, S-CH_2), 2.19 (m, 4H, cyclohexyl CH_2), 1.98 (d, *J* = 12.7 Hz, 2H, cyclohexyl CH_2), 1.81–1.71 (m, 3H, cyclohexyl CH_2), 1.54–1.40 (m, 2H, CH_2), 1.37–1.30 (m, 1H, cyclohexyl CH_2), 0.99 (t, *J* = 5.6 Hz, 3H, CH_3). ^{13}C NMR (100 MHz, $CDCl_3$) δ 169.0, 158.0, 152.6, 150.6, 148.5, 131.6, 130.8, 122.9, 119.1, 117.9, 117.7, 57.8, 33.2, 32.1, 25.5, 25.3, 22.7, 13.6. HR-MS (ESI): Calcd. $C_{20}H_{25}N_7OS$, $[M+H]^+$m/z: 412.1914, found: 412.1917.

*4.5.4 4-chloro-2-((2-(3-cyclohexyl-5-(propylthio)-3H-[1,2,3]triazolo[4,5-d]pyrimidin-7-yl)hydrazono)methyl)phenol (**8**)*

White solid, yield: 85%; m.p.: 243–246 °C. IR (KBr) cm^{-1}, 3378 (OH), 3241 (NH), 3031 (CH-Ar), 2965 (CH), 2926 (CH), 2854 (CH), 1580 (C=N). ^{1}H NMR (400 MHz, DMSO-d_6) δ 12.71 (s, 1H, OH), 11.08 (s, 1H, NH), 8.40 (s, 1H, N=CH), 7.68–7.61 (m, 1H, ArH), 7.34 (dd, *J* = 8.7, 2.6 Hz, 1H, ArH), 6.98 (d, *J* = 8.8 Hz, 1H, ArH), 4.72 (s, 1H, N-CH), 3.17–3.11 (m, 2H, S-CH_2), 2.13–2.04 (m, 4H, cyclohexyl CH_2), 1.93–1.85 (m, 2H, cyclohexyl CH_2), 1.75 (dd, *J* = 14.5, 7.4 Hz, 3H, cyclohexyl CH_2), 1.56–1.44 (m, 2H, CH_2), 1.34–1.26 (m, 1H, cyclohexyl CH_2), 1.03 (t, *J* = 7.3 Hz, 3H, CH_3). ^{13}C NMR (100 MHz, DMSO-d_6) δ 168.2. 159.0, 151.8, 150.2, 149.0, 132.3, 122.2, 106.4, 103.7, 97.9, 57.1, 43.8, 32.3, 31.4, 24.8, 22.5, 13.4, 12.5. HR-MS (ESI): Calcd. $C_{20}H_{24}ClN_7OS$, $[M+Na]^+$m/z: 468.1344, found: 468.1342.

*4.5.5 2-((2-(3-cyclohexyl-5-(propylthio)-3H-[1,2,3]triazolo[4,5-d]pyrimidin-7-yl)hydrazono)methyl)-5-(diethylamino)phenol (**9**)*

Yellow solid, yield: 77%; m.p.: 200–201 °C. IR (KBr) cm^{-1}, 3421 (OH), 3170 (NH), 3093 (CH-Ar), 2966, (CH), 2930 (CH), 2856 (CH), 1584 (C=N). ^{1}H NMR (400 MHz, DMSO-d_6) δ 12.31 (s, 1H, OH), 11.04 (s, 1H, NH), 8.23 (s, 1H, N=CH), 7.13 (d, *J* = 8.7 Hz, 1H, ArH), 6.27 (d, *J* = 8.6 Hz, 1H, ArH), 6.16–6.12 (m, 1H, ArH), 4.74–4.64 (m, 1H, N-CH), 3.41–3.33 (m, 4H, 2-N-CH_2), 3.12 (t, *J* = 7.1 Hz, 2H, S-CH_2), 2.16–2.02 (m, 4H, cyclohexyl CH_2), 1.94–1.84 (m, 2H, cyclohexyl CH_2), 1.80–1.69 (m, 3H, cyclohexyl CH_2), 1.58–1.43 (m, 2H, CH_2), 1.37–1.20 (m, 1H, cyclohexyl CH_2), 1.12 (t, *J* = 6.8 Hz, 6H, 2-CH_3), 1.02 (t, *J* = 7.3 Hz, 3H, CH_3).

^{13}C NMR (100 MHz, DMSO-d_6) δ 168.2, 159.0, 151.8, 150.2, 149.0, 132.3, 122.2, 106.4, 103.7, 97.9, 57.1, 43.8, 32.3, 31.4, 24.9, 24.8, 22.5, 13.4, 12.5. HR-MS (ESI): Calcd. $C_{24}H_{34}N_8OS$, $[M+H]^+$m/z: 483.2649, found: 483.2655.

*4.5.6 2-((2-(3-cyclohexyl-5-(propylthio)-3H-[1,2,3]triazolo[4,5-d]pyrimidin-7-yl)hydrazono)methyl)-5-methoxyphenol (**10**)*

White solid, yield: 78%; m.p.: 189–192 °C. IR (KBr) cm^{-1}, 3387 (OH), 3161 (NH), 3065 (CH-Ar), 2962, (CH), 2925 (CH), 2853 (CH), 1565 (C=N). ^{1}H NMR (400 MHz, DMSO-d_6) δ 12.49 (s, 1H, OH), 11.21 (s, 1H, NH), 8.34 (s, 1H, N=CH), 7.35 (d, J = 8.5 Hz, 1H, ArH), 6.57–6.48 (m, 2H, ArH), 4.77–4.64 (m, 1H, N-CH), 3.79 (s, 3H, O-CH_3), 3.13 (t, J = 7.0 Hz, 2H, S-CH_2), 2.09 (s, 4H, cyclohexyl CH_2), 1.89 (d, J = 12.7 Hz, 2H, cyclohexyl CH_2), 1.80–1.66 (m, 3H, cyclohexyl CH_2), 1.57–1.44 (m, 2H, CH_2), 1.32 (t, J = 12.1 Hz, 1H, cyclohexyl CH_2), 1.02 (t, J = 7.2 Hz, 3H, CH_3). ^{13}C NMR (100 MHz, DMSO-d_6) δ 168.4, 162.1, 158.8, 152.2, 150.1, 148.3, 132.3, 122.2, 111.5, 106.4, 101.6, 57.2, 55.3, 32.3, 31.4, 24.9, 24.7, 22.5, 13.3. HR-MS (ESI): Calcd. $C_{21}H_{27}N_7O_2S$, $[M+H]^+$m/z: 442.2020, found: 442.2025.

*4.5.7 2-((2-(3-cyclohexyl-5-(propylthio)-3H-[1,2,3]triazolo[4,5-d]pyrimidin-7-yl)hydrazono)methyl)-6-ethoxyphenol (**11**)*

White solid, yield: 80%; m.p.: 121–123°C. IR (KBr) cm^{-1}, 3399 (OH), 3121 (NH), 3023 (CH-Ar), 2958, (CH), 2935 (CH), 2862 (CH), 1562 (C=N). ^{1}H NMR (400 MHz, DMSO-d_6) δ 12.61 (s, 1H, OH), 10.98 (s, 1H, NH), 8.40 (s, 1H, N=CH), 7.03 (d, J = 7.9 Hz, 2H, ArH), 6.86 (t, J = 7.9 Hz, 1H, ArH), 4.77–4.66 (m, 1H, N-CH), 4.10–4.04 (m, 2H, O-CH_2), 3.14 (t, J = 7.2 Hz, 2H, S-CH_2), 2.14–2.04 (m, 4H, cyclohexyl CH_2), 1.90 (d, J = 13.2 Hz, 2H, cyclohexyl CH_2), 1.78–1.70 (m, 3H, cyclohexyl CH_2), 1.58–1.46 (m, 2H, CH_2), 1.38 (t, J = 6.9 Hz, 3H, CH_3), 1.34–1.25 (m, 1H, cyclohexyl CH_2), 1.03 (t, J = 7.3 Hz, 3H, CH_3). ^{13}C NMR (100 MHz, DMSO-d_6) δ 168.5, 152.3, 149.6, 148.4, 147.3, 147.0, 122.5, 122.3, 118.9, 118.2, 115.3, 64.0, 57.1, 32.3, 31.5, 24.9, 24.7, 22.5, 14.8, 13.3. HR-MS (ESI): Calcd. $C_{22}H_{29}N_7O_2S$, $[M+Na]^+$m/z: 478.1996, found: 478.2002.

4.5.8 3-cyclohexyl-5-(propylthio)-7-(2-(pyridin-2-ylmethylene)hydrazinyl)-3H-

*[1,2,3]triazolo[4,5-d]pyrimidine (**12**)*

White solid, yield: 80%; m.p.: 233–235 °C. IR (KBr) cm^{-1}, 3172 (NH), 3045 (CH-Ar), 2926 (CH), 2862 (CH), 1562 (C=N). ^1H NMR (400 MHz, DMSO-d_6) δ 12.61 (s, 1H, NH), 8.62 (d, J = 4.6 Hz, 1H, ArH), 8.31 (s, 1H, N=CH), 8.24–8.19 (m, 1H, ArH), 7.94 (t, J = 7.4 Hz, 1H, ArH), 7.45–7.40 (m, 1H, ArH), 4.76–4.69 (m, 1H, N-CH), 3.15 (t, J = 7.2 Hz, 2H, S-CH_2), 2.17–2.03 (m, 4H, cyclohexyl CH_2), 1.90 (d, J = 13.3 Hz, 2H, cyclohexyl CH_2), 1.82–1.69 (m, 3H, cyclohexyl CH_2), 1.57–1.49 (m, 2H, CH_2), 1.32–1.29 (m, 1H, cyclohexyl CH_2), 1.03 (t, J = 7.3 Hz, 3H, CH_3). ^{13}C NMR (100 MHz, DMSO-d_6) δ 153.3, 149.4, 136.8, 124.2, 119.9, 57.1, 32.4, 31.5, 24.9, 24.8, 22.5, 13.4. HR-MS (ESI): Calcd. $C_{19}H_{24}N_8S$, $[M+H]^+$m/z: 397.1917, found: 397.1920.

*4.5.9 7-(2-((2-chloropyridin-3-yl)methylene)hydrazinyl)-3-cyclohexyl-5-(propylthio)-3H-[1,2,3]triazolo[4,5-d]pyrimidine (**13**)*

White solid, yield: 82%; m.p.: 233–235 °C. IR (KBr) cm^{-1}, 3172 (NH), 3045 (CH-Ar), 2926 (CH), 2862 (CH), 1562 (C=N). ^1H NMR (400 MHz, $CDCl_3$) δ 9.91 (s, 1H, NH), 8.77–8.70 (m, 1H, ArH), 8.44 (s, 1H, N=CH), 8.41 (dd, J = 4.7, 2.0 Hz, 1H, ArH), 7.35 (dd, J = 7.8, 4.7 Hz, 1H, ArH), 4.80–4.69 (m, 1H, N-CH), 3.19 (t, J = 7.3 Hz, 2H, S-CH_2), 2.26–2.12 (m, 4H, cyclohexyl CH_2), 1.98 (d, J = 13.5 Hz, 2H, cyclohexyl CH_2), 1.85–1.78 (m, 3H, cyclohexyl CH_2), 1.54–1.51 (m, 2H, CH_2), 1.39–1.35 (m, 1H, cyclohexyl CH_2), 1.08 (t, J = 7.4 Hz, 3H, CH_3). ^{13}C NMR (100 MHz, $CDCl_3$) δ 150.5, 150.1, 136.7, 128.6, 125.0, 123.2, 58.0, 33.4, 32.1, 25.5, 25.3, 22.8, 13.6. HR-MS (ESI): Calcd. $C_{19}H_{23}ClN_8S$, $[M+Na]^+$m/z: 453.1347, found: 453.1350.

*4.5.10 3-cyclohexyl-7-(2-(furan-2-ylmethylene)hydrazinyl)-5-(propylthio)-3H-[1,2,3]triazolo[4,5-d]pyrimidine (**14**)*

Yellow solid, yield: 79%; m.p.: 136–138 °C. IR (KBr) cm^{-1}, 3164 (NH), 3094 (CH-Ar), 2958 (CH), 2930 (CH), 2854 (CH), 1542 (C=N). ^1H NMR (400 MHz, $CDCl_3$) δ 10.51 (s, 1H, NH), 8.24 (s, 1H, N=CH), 7.55–7.52 (m, 1H, ArH), 6.84 (d, J = 3.4 Hz, 1H, ArH), 6.49 (dd, J = 3.2, 1.7 Hz, 1H, ArH), 4.74–4.70 (m, 1H, N-CH), 3.16 (t, J = 7.1 Hz, 2H, S-CH_2), 2.20–2.14

(m, 4H, cyclohexyl CH_2), 1.96 (d, J = 13.5 Hz, 2H, cyclohexyl CH_2), 1.82–1.76 (m, 3H, cyclohexyl CH_2), 1.57–1.44 (m, 2H, CH_2), 1.40–1.33 (m, 1H, cyclohexyl CH_2), 1.05 (t, J = 7.3 Hz, 3H, CH_3). ^{13}C NMR (100 MHz, $CDCl_3$) δ 149.4, 148.8, 144.8, 130.0, 122.7, 116.1, 113.3, 112.1, 112.0, 58.3, 57.9, 33.3, 32.1, 25.5, 25.4, 25.2, 22.8, 13.6. HR-MS (ESI): Calcd. $C_{18}H_{23}N_7OS$, $[M+Na]^+$m/z: 408.1577, found: 408.1581.

*4.5.11 3-cyclohexyl-5-(propylthio)-7-(2-(thiophen-2-ylmethylene)hydrazinyl)-3H-[1,2,3]triazolo[4,5-d]pyrimidine (**15**)*

White solid, yield: 78%; m.p.: 190–192 °C. IR (KBr) cm^{-1}, 3229 (NH), 3086 (CH-Ar), 2957 (CH), 2932 (CH), 2855 (CH), 1583 (C=N). ^{1}H NMR (400 MHz, $CDCl_3$) δ 8.42 (s, 1H, N=CH), 7.42 (d, J = 5.0 Hz, 1H, ArH), 7.33 (d, J = 3.0 Hz, 1H, ArH), 7.07 (dd, J = 4.9, 3.7 Hz, 1H, ArH), 4.74–4.71 (m, 1H, N-CH), 3.20 (t, J = 6.9 Hz, 2H, S-CH_2), 2.25–2.12 (m, 4H, cyclohexyl CH_2), 1.96 (d, J = 13.4 Hz, 2H, cyclohexyl CH_2), 1.86–1.77 (m, 3H, cyclohexyl CH_2), 1.55–1.46 (m, 2H, CH_2), 1.40–1.33 (m, 1H, cyclohexyl CH_2), 1.08 (t, J = 7.3 Hz, 3H, CH_3). ^{13}C NMR (100 MHz, $CDCl_3$) δ 138.8, 129.8, 128.9, 127.5, 57.8, 33.4, 32.2, 25.4, 25.2, 22.9, 13.6. HR-MS (ESI): Calcd. $C_{18}H_{23}N_7S_2$, $[M+H]^+$m/z: 402.1529, found: 402.1533.

*4.5.12 3-cyclohexyl-7-(2-(1-phenylethylidene)hydrazinyl)-5-(propylthio)-3H-[1,2,3]triazolo[4,5-d]pyrimidine (**16**)*

White solid, yield: 84%; m.p.: 158–160 °C. IR (KBr) cm^{-1}, 3345 (NH), 3045 (CH-Ar), 2961 (CH), 2939 (CH), 2854 (CH), 1576 (C=N). ^{1}H NMR (400 MHz, DMSO-d_6) δ 11.49 (s, 1H, NH), 8.15–8.10 (m, 2H, ArH), 7.49–7.42 (m, 3H, ArH), 4.78–4.65 (m, 1H, N-CH), 3.16 (t, J = 7.1 Hz, 2H, S-CH_2), 2.43 (s, 3H, CH_3), 2.14–2.08 (m, 4H, cyclohexyl CH_2), 1.90 (d, J = 12.8 Hz, 2H, cyclohexyl CH_2), 1.78–1.73 (m, 3H, cyclohexyl CH_2), 1.53–1.44 (m, 2H, CH_2), 1.33–1.28 (m, 1H, cyclohexyl CH_2), 1.03 (t, J = 7.3 Hz, 3H, CH_3). ^{13}C NMR (100 MHz, DMSO-d_6) δ 168.0, 154.1, 151.2, 150.7, 137.9, 129.2, 128.2, 126.5, 122.6, 57.1, 32.3, 31.5, 24.9, 24.8, 22.5, 13.3. HR-MS (ESI): Calcd. $C_{21}H_{27}N_7S$, $[M+H]^+$m/z: 410.2121, found: 410.2126.

*4.5.13 3-(1-(2-(3-cyclohexyl-5-(propylthio)-3H-[1,2,3]triazolo[4,5-d]pyrimidin-7-yl)hydrazono)ethyl)aniline (**17**)*

Yellow solid, yield: 73%; m.p.: 199–202 °C. IR (KBr) cm^{-1}, 3412 (NH), 3331 (NH), 3264 (NH), 3038 (CH-Ar), 2959 (CH), 2939 (CH), 2851 (CH), 1539 (C=N) ^{1}H NMR (400 MHz, DMSO-d_6) δ 11.33 (s, 1H, NH), 7.38–7.35 (m, 1H, ArH), 7.18–7.12 (m, 1H, ArH), 7.10 (t, J = 7.8 Hz, 1H, ArH), 6.64 (d, J = 7.7 Hz, 1H, ArH), 5.13 (s, 2H, NH_2), 4.75–4.65 (m, 1H, N-CH), 3.15 (t, J = 7.1 Hz, 2H, S-CH_2), 2.36 (s, 3H, CH_3), 2.19–2.03 (m, 4H, cyclohexyl CH_2), 1.89 (d, J = 12.6 Hz, 2H, cyclohexyl CH_2), 1.80–1.72 (m, 3H, cyclohexyl CH_2), 1.50 (d, J = 8.3 Hz, 2H, CH_2), 1.34–1.28 (m, 1H, cyclohexyl CH_2), 1.03 (t, J = 7.3 Hz, 3H, CH_3). ^{13}C NMR (100 MHz, DMSO-d_6) δ 168.0, 150.4, 148.4, 138.5, 128.7, 122.5, 118.4, 115.0, 114.6, 112.2, 57.1, 32.3, 31.5, 24.9, 24.8, 22.5, 13.3. HR-MS (ESI): Calcd. $C_{21}H_{28}N_8S$, $[M+Na]^+$m/z: 447.2050, found: 447.2057.

*4.5.14 7-(2-(1-(4-chlorophenyl)ethylidene)hydrazinyl)-3-cyclohexyl-5-(propylthio)-3H-[1,2,3]triazolo[4,5-d]pyrimidine (**18**)*

Yellow solid, yield: 80%; m.p.: 232–234 °C. IR (KBr) cm^{-1}, 3163 (NH), 3024 (CH-Ar), 2965 (CH), 2930 (CH), 2858 (CH), 1562 (C=N). ^{1}H NMR (400 MHz, DMSO-d_6) δ 11.56 (s, 1H, NH), 8.15 (d, J = 7.6 Hz, 2H, ArH), 7.54–7.52 (m, 1H, ArH), 7.51–7.49 (m, 1H, ArH), 4.75–4.68 (m, 1H, N-CH), 3.16 (t, J = 7.2 Hz, 2H, S-CH_2), 2.41 (s, 3H, CH_3), 2.13–2.07 (m, 4H, cyclohexyl CH_2), 1.90 (d, J = 13.0 Hz, 2H, cyclohexyl CH_2), 1.78–1.73 (m, 3H, cyclohexyl CH_2), 1.56–1.45 (m, 2H, CH_2), 1.35–1.29 (m, 1H, cyclohexyl CH_2), 1.03 (t, J = 7.3 Hz, 3H, CH_3). ^{13}C NMR (100 MHz, DMSO-d_6) δ 168.0, 154.0, 150.4, 136.8, 133.9, 128.3, 128.2, 122.6, 57.1, 32.3, 31.5, 24.9, 24.8, 22.5, 13.3. HR-MS (ESI): Calcd. $C_{21}H_{26}ClN_7S$, $[M+H]^+$m/z: 444.1732, found: 444.1736.

*4.5.15 2-(1-(2-(3-cyclohexyl-5-(propylthio)-3H-[1,2,3]triazolo[4,5-d]pyrimidin-7-yl)hydrazono)ethyl)phenol (**19**)*

Yellow solid, yield: 83%; m.p.: 181–183 °C. IR (KBr) cm^{-1}, 3422 (OH), 3175 (NH), 3050 (CH-Ar), 2960 (CH), 2929 (CH), 2859 (CH), 1570 (C=N). ^{1}H NMR (400 MHz, DMSO-d_6) δ 11.73 (s, 1H, OH), 11.65 (s, 1H, NH), 7.65 (d, J = 7.6 Hz, 1H, ArH), 7.31 (t, J = 7.4 Hz, 1H, ArH), 6.96–6.89 (m, 2H, ArH), 4.80–4.67 (m, 1H, N-CH), 3.16 (t, J = 6.9 Hz, 2H, S-CH_2), 2.52 (s, 3H, CH_3), 2.11 (d, J = 2.9 Hz, 4H, cyclohexyl CH_2), 1.90 (d, J = 13.2 Hz, 2H, cyclohexyl

CH_2), 1.78–1.73 (m, 3H, cyclohexyl CH_2), 1.58–1.45 (m, 2H, CH_2), 1.35–1.29 (m, 1H, cyclohexyl CH_2), 1.03 (t, J = 7.3 Hz, 3H, CH_3). ^{13}C NMR (100 MHz, DMSO-d_6) δ 168.2, 157.0, 154.0, 152.9, 150.2, 131.1, 128.9, 122.2, 120.0, 118.8, 117.6, 57.3, 32.3, 31.4, 24.8, 24.7, 22.5, 14.5, 13.3. HR-MS (ESI): Calcd. $C_{21}H_{27}N_7OS$, $[M+Na]^+$m/z: 448.1890, found: 448.1897.

*4.5.16 3-(1-(2-(3-cyclohexyl-5-(propylthio)-3H-[1,2,3]triazolo[4,5-d]pyrimidin-7-yl)hydrazono)ethyl)phenol (**20**)*

White solid, yield: 81%; m.p.: 247–250 °C. IR (KBr) cm^{-1}, 3390 (OH), 3142 (NH), 3031 (CH-Ar), 2961 (CH), 2931 (CH), 2867 (CH), 1574 (C=N). ^{1}H NMR (400 MHz, DMSO-d_6) δ 11.42 (s, 1H, NH), 9.52 (s, 1H, OH), 7.60–7.52 (m, 1H, ArH), 7.50–7.46 (m, 1H, ArH), 7.24 (t, J = 7.9 Hz, 1H, ArH), 6.84 (dd, J = 8.0, 1.9 Hz, 1H, ArH), 4.75–4.68 (m, 1H, N-CH), 3.16 (t, J = 7.0 Hz ,2H, S-CH_2), 2.38 (s, 3H, CH_3), 2.16–2.08 (m, 4H, cyclohexyl CH_2), 1.90 (d, J = 13.2 Hz, 2H, cyclohexyl CH_2), 1.79–1.73 (m, 3H, cyclohexyl CH_2), 1.53–1.49 (m, 2H, CH_2), 1.35–1.28 (m, 1H, cyclohexyl CH_2), 1.03 (t, J = 7.3 Hz, 3H, CH_3). ^{13}C NMR (100 MHz, DMSO-d_6) δ 168.0, 161.5, 157.3, 154.2, 139.3, 129.1, 124.5, 122.5, 117.5, 116.3, 113.4, 57.1, 32.3, 31.5, 24.9, 24.8, 22.5, 13.3. HR-MS (ESI): Calcd. $C_{21}H_{27}N_7OS$, $[M+H]^+$m/z: 426.2071, found: 426.2078.

*4.5.17 4-(1-(2-(3-cyclohexyl-5-(propylthio)-3H-[1,2,3]triazolo[4,5-d]pyrimidin-7-yl)hydrazono)ethyl)phenol (**21**)*

Yellow solid, yield: 79%; m.p.: 115–117 °C. IR (KBr) cm^{-1}, 3380 (OH), 3125 (NH), 3020 (CH-Ar), 2963 (CH), 2931 (CH), 2850 (CH), 1562 (C=N). ^{1}H NMR (400 MHz, DMSO-d_6) δ 11.33 (s, 1H, NH), 9.78 (s, 1H, OH), 7.96–7.84 (m, 2H, ArH), 6.83 (d, J = 8.2 Hz, 2H, ArH), 4.77–4.63 (m, 1H, N-CH), 3.15 (t, J = 7.2 Hz, 2H, S-CH_2), 2.36 (s, 3H, CH_3), 2.12–2.03 (m, 4H, cyclohexyl CH_2), 1.89 (d, J = 12.9 Hz, 2H, cyclohexyl CH_2), 1.80–1.71 (m, 3H, cyclohexyl CH_2), 1.54–1.47 (m, 2H, CH_2), 1.40–1.20 (m, 1H, cyclohexyl CH_2), 1.03 (t, J = 7.3 Hz, 3H, CH_3). ^{13}C NMR (100 MHz, DMSO-d_6) δ 167.9, 162.0, 158.7, 150.4, 130.7, 128.8, 128.6, 128.2, 122.5, 115.1, 57.0, 32.3, 31.5, 26.2, 24.9, 24.8, 22.6. HR-MS (ESI): Calcd. $C_{21}H_{27}N_7OS$, $[M+Na]^+$m/z: 448.1890, found: 448.1891.

*4.5.18 2-(1-(2-(3-cyclohexyl-5-(propylthio)-3H-[1,2,3]triazolo[4,5-d]pyrimidin-7-yl)hydrazono)ethyl)benzene-1,4-diol (**22**)*

Yellow solid, yield: 84%; m.p.: 246–247 °C. IR (KBr) cm^{-1}, 3323 (OH), 3210 (NH), 3021 (CH-Ar), 2931 (CH), 2858 (CH), 1546 (C=N). ^{1}H NMR (400 MHz, DMSO-d_6) δ 11.62 (s, 1H, NH), 11.10 (s, 1H, OH), 8.96–8.92 (m, 1H, ArH), 7.02–6.95 (m, 1H, ArH), 6.79–6.74 (m, 2H, ArH), 4.81–4.69 (m, 1H, N-CH), 3.16 (t, J = 7.1 Hz, 2H, S-CH_2), 2.46 (s, 3H, CH_3), 2.14–2.06 (m, 4H, cyclohexyl CH_2), 1.89 (d, J = 13.2 Hz, 2H, cyclohexyl CH_2), 1.78–1.73 (m, 3H, cyclohexyl CH_2), 1.59–1.42 (m, 2H, CH_2), 1.35–1.29 (m, 1H, cyclohexyl CH_2), 1.03 (t, J = 7.3 Hz, 3H, CH_3). ^{13}C NMR (100 MHz, DMSO-d_6) δ 167.5, 152.3, 149.4, 149.3, 124.5, 120.4, 119.3, 117.7, 114.5, 114.2, 57.3, 32.3, 31.4, 24.9, 24.7, 22.5, 14.9, 14.5, 13.3. HR-MS (ESI): Calcd. $C_{21}H_{27}N7O_2S$, $[M+H]^+$m/z: 442.2020, found: 442.2018.

*4.5.19 4-chloro-2-(1-(2-(3-cyclohexyl-5-(propylthio)-3H-[1,2,3]triazolo[4,5-d]pyrimidin-7-yl)hydrazono)ethyl)phenol (**23**)*

Yellow solid, yield: 91%; m.p.: 93–95 °C. IR (KBr) cm^{-1}, 3470 (OH), 3172 (NH), 3025 (CH-Ar), 2932 (CH), 2856 (CH), 1548 (C=N). ^{1}H NMR (400 MHz, $CDCl_3$) δ 11.76 (s, 1H, NH), 8.88 (s, 1H, OH), 7.26–7.22 (m, 1H, ArH), 7.14–7.12 (m, 1H, ArH), 6.95 (d, J = 8.5 Hz, 1H, ArH), 4.75–4.66 (m, 1H, N-CH), 3.15 (t, J = 7.3 Hz, 2H, S-CH_2), 2.36 (s, 3H, CH_3), 2.21–2.11 (m, 4H, cyclohexyl CH_2), 1.97 (d, J = 13.3 Hz, 2H, cyclohexyl CH_2), 1.85–1.78 (m, 3H, cyclohexyl CH_2), 1.56–1.46 (m, 2H, CH_2), 1.42–1.32 (m, 1H, cyclohexyl CH_2), 1.08 (t, J = 7.3 Hz, 3H, CH_3). ^{13}C NMR (100 MHz, $CDCl_3$) δ 169.4, 156.4, 152.2, 151.8, 150.7, 130.8, 127.1, 123.2, 122.3, 120.5, 119.9, 57.9, 33.3, 32.2, 25.5, 25.3, 22.8, 13.6, 12.4. HR-MS (ESI): Calcd. $C_{21}H_{26}ClN_7OS$, $[M+Na]^+$m/z: 482.1500, found: 482.1502.

*4.5.20 2-amino-6-(1-(2-(3-cyclohexyl-5-(propylthio)-3H-[1,2,3]triazolo[4,5-d]pyrimidin-7-yl)hydrazono)ethyl)phenol (**24**)*

Yellow solid, yield: 88%; m.p.: 236–238 °C. IR (KBr) cm^{-1}, 3439 (OH), 3395 (NH), 3326 (NH), 3025 (CH-Ar), 2930 (CH), 2854 (CH), 1544 (C=N). ^{1}H NMR (400 MHz, DMSO-d_6) δ 13.41 (s, 1H, OH), 11.92 (s, 1H, NH), 7.15–7.10 (m, 1H, ArH), 6.94–6.69 (m, 1H, ArH), 6.79–

6.73 (m, 1H, ArH), 6.26 (bs, 2H, NH_2), 4.77–4.70 (m, 1H, N-CH), 3.17 (t, *J* = 6.7 Hz, 2H, S-CH_2), 2.54 (s, 3H, CH_3), 2.16–2.04 (m, 4H, cyclohexyl CH_2), 1.90 (d, *J* = 12.8 Hz, 2H, cyclohexyl CH_2), 1.79–1.73 (m, 3H, cyclohexyl CH_2), 1.53–1.50 (m, 2H, CH_2), 1.36–1.29 (m, 1H, cyclohexyl CH_2), 1.03 (t, *J* = 7.3 Hz, 3H, CH_3). ^{13}C NMR (100 MHz, DMSO-d_6) δ 168.8, 152.8, 147.6, 136.3, 118.9, 118.7, 117.7, 117.5, 117.2, 57.3, 32.3, 31.5, 24.9, 24.8, 22.4, 14.7, 13.3. HR-MS (ESI): Calcd. $C_{21}H_{28}N_8OS$, $[M+H]^+$m/z: 441.2180, found: 441.2184.

*4.5.21 3-benzyl-5-(propylthio)-7-(2-(pyridin-2-ylmethylene)hydrazinyl)-3H-[1,2,3]triazolo[4,5-d]pyrimidine (**25**)*

White solid, yield: 79%; m.p.: 233–234 °C. IR (KBr) cm^{-1}, 3107 (NH), 3025 (CH-Ar), 2965 (CH), 2930 (CH), 2871 (CH), 1561 (C=N). ^{1}H NMR (400 MHz, DMSO-d_6) δ 12.65 (s, 1H, NH), 8.62 (d, *J* = 4.5 Hz, 1H, ArH), 8.31 (s, 1H, N=CH), 8.25–8.19 (m, 1H, ArH), 7.93 (t, *J* = 7.2 Hz, 1H, ArH), 7.46–7.40 (m, 1H, ArH), 7.41–7.29 (m, 5H, ArH), 5.77 (s, 2H, N-CH_2), 3.15 (t, *J* = 7.1 Hz, 2H, S-CH_2), 1.79–1.65 (m, 2H, CH_2), 1.01 (t, *J* = 7.3 Hz, 3H, CH_3). ^{13}C NMR (100 MHz, DMSO-d_6) δ 153.2, 149.5, 146.6, 136.8, 135.6, 128.7, 128.1, 128.0, 124.3, 119.9, 49.4, 32.3, 22.4, 13.3. HR-MS (ESI): Calcd. $C_{20}H_{20}N_8S$, $[M+Na]^+$m/z: 427.1424, found: 427.1425.

*4.5.22 3-(4-chlorobenzyl)-5-(propylthio)-7-(2-(pyridin-2-ylmethylene)hydrazinyl)-3H-[1,2,3]triazolo[4,5-d]pyrimidine (**26**)*

White solid, yield: 83%; m.p.: 249–250 °C. IR (KBr) cm^{-1}, 3118 (NH), 3065 (CH-Ar), 2966 (CH), 2930 (CH), 2871 (CH), 1561 (C=N). ^{1}H NMR (400 MHz, DMSO-d_6) δ 12.67 (s, 1H, NH), 8.62 (d, *J* = 4.4 Hz, 1H, ArH), 8.31 (s, 1H, N=CH), 8.25–8.18 (m, 1H, ArH), 7.94 (t, *J* = 7.2 Hz, 1H, ArH), 7.48–7.35 (m, 5H, ArH), 5.78 (s, 2H, N-CH_2), 3.13 (t, *J* = 7.0 Hz, 2H, S-CH_2), 1.75–1.65 (m, 2H, CH_2), 1.00 (t, *J* = 7.3 Hz, 3H, CH_3). ^{13}C NMR (100 MHz, DMSO-d_6) δ 153.2, 149.5, 136.8, 134.6, 132.7, 129.9, 128.7, 124.3, 119.9, 48.7, 32.3, 28.3, 22.4, 13.3. HR-MS (ESI): Calcd. $C_{20}H_{19}ClN_8S$, $[M+Na]^+$m/z: 461.1034, found: 461.1035.

*4.5.23 3-(4-isopropylbenzyl)-5-(propylthio)-7-(2-(pyridin-2-ylmethylene)hydrazinyl)-3H-[1,2,3]triazolo[4,5-d]pyrimidine (**27**)*

Yellow solid, yield: 94%; m.p.: 214–216 °C. IR (KBr) cm^{-1}, 3120 (NH), 3032 (CH-Ar), 2957 (CH), 2930 (CH), 2870 (CH), 1562 (C=N). ^{1}H NMR (400 MHz, DMSO-d_6) δ 12.65 (s, 1H, NH), 8.62 (d, J = 4.6 Hz, 1H, ArH), 8.31 (s, 1H, N=CH), 8.25–8.17 (m, 1H, ArH), 7.93 (t, J = 7.4 Hz, 1H, ArH), 7.45–7.39 (m, 1H, ArH), 7.31 (d, J = 8.0 Hz, 2H, ArH), 7.23 (d, J = 8.1 Hz, 2H, ArH), 5.71 (s, 2H, N-CH_2), 3.15 (t, J = 7.1 Hz, 2H, S-CH_2), 2.90–2.81 (m, 1H, CH), 1.79–1.66 (m, 2H, CH_2), 1.16 (d, J = 6.9 Hz, 6H, 2-CH_3), 1.01 (t, J = 7.3 Hz, 3H, CH_3). ^{13}C NMR (100 MHz, DMSO-d_6) δ 153.2, 149.5, 148.3, 136.8, 133.0, 128.6, 128.1, 126.6, 124.3, 119.9, 49.3, 38.1, 33.1, 23.7, 22.4, 13.3. HR-MS (ESI): Calcd. $C_{23}H_{26}N_8S$, $[M+Na]^+$m/z: 469.1893, found: 469.1892.

*4.5.24 3-(furan-2-ylmethyl)-5-(propylthio)-7-(2-(pyridin-2-ylmethylene)hydrazinyl)-3H-[1,2,3]triazolo[4,5-d]pyrimidine (**28**)*

White solid, yield: 82%; m.p.: 220–222 °C. IR (KBr) cm^{-1}, 3120 (NH), 3020 (CH-Ar), 2962 (CH), 2930 (CH), 2873 (CH), 1562 (C=N). ^{1}H NMR (400 MHz, DMSO-d_6) δ 12.65 (s, 1H, NH), 8.62 (d, J = 4.5 Hz, 1H, ArH), 8.31 (s, 1H, N=CH), 8.25–8.17 (m, 1H, ArH), 7.93 (t, J = 7.3 Hz, 1H, ArH), 7.64 (d, J = 0.9 Hz, 1H, ArH), 7.47–7.38 (m, 1H, ArH), 6.58–6.55 (m, 1H, ArH), 6.50–6.43 (m, 1H, ArH), 5.79 (s, 2H, N-CH_2), 3.17 (t, J = 7.1 Hz, 2H, S-CH_2), 1.83–1.68 (m, 2H, CH_2), 1.03 (t, J = 7.3 Hz, 3H, CH_3). ^{13}C NMR (100 MHz, DMSO-d_6) δ 153.2, 149.5, 148.1, 146.6, 143.5, 136.8, 124.2, 119.9, 110.8, 109.7, 42.5, 32.3, 22.3, 13.3. HR-MS (ESI): Calcd. $C_{18}H_{18}N_8OS$, $[M+Na]^+$m/z: 417.1216, found: 417.1215.

*4.5.25 5-(propylthio)-7-(2-(pyridin-2-ylmethylene)hydrazinyl)-3-(2-(thiophen-2-yl)ethyl)-3H-[1,2,3]triazolo[4,5-d]pyrimidine (**29**)*

White solid, yield: 81%; m.p.: 197–199 °C. IR (KBr) cm^{-1}, 3150 (NH), 3075 (CH-Ar), 2966 (CH), 2929 (CH), 2855 (CH), 1568 (C=N). ^{1}H NMR (400 MHz, DMSO-d_6) δ 12.63 (s, 1H, NH), 8.62 (d, J = 4.5 Hz, 1H, ArH), 8.30 (s, 1H, N=CH), 8.24–8.17 (m, 1H, ArH), 7.94 (t, J = 7.5 Hz, 1H, ArH), 7.46–7.38 (m, 1H, ArH), 7.29 (d, J = 4.5 Hz, 1H, ArH), 6.91–6.84 (m, 1H, ArH), 6.80 (d, J = 2.8 Hz, 1H, ArH), 4.79 (t, J = 6.7 Hz, 2H, N-CH_2), 3.55 (t, J = 6.6 Hz, 2H, CH_2), 3.14 (t, J = 7.2 Hz, 2H, S-CH_2), 1.80–1.67 (m, 2H, CH_2), 1.02 (t, J = 7.3 Hz, 3H, CH_3). ^{13}C NMR (100 MHz, DMSO-d_6) δ 153.2, 149.5, 139.3, 136.8, 127.0, 125.9, 124.7, 124.2,

120.0, 47.5, 32.3, 28.5, 22.4, 13.4. HR-MS (ESI): Calcd. $C_{19}H_{20}N_8S_2$, $[M+Na]^+$m/z: 447.1145, found: 447.1146.

*4.5.26 3-isobutyl-5-(propylthio)-7-(2-(pyridin-2-ylmethylene)hydrazinyl)-3H-[1,2,3]triazolo[4,5-d]pyrimidine (**30**)*

White solid, yield: 82%; m.p.: 220–222 °C. IR (KBr) cm^{-1}, 3158 (NH), 3012 (CH-Ar), 2962 (CH), 2932 (CH), 2871 (CH), 1574 (C=N). ^{1}H NMR (400 MHz, DMSO-d_6) δ 12.63 (s, 1H, NH), 8.63 (d, J = 4.6 Hz, 1H, ArH), 8.32 (s, 1H, N=CH), 8.27–8.18 (m, 1H, ArH), 7.94 (t, J = 7.5 Hz, 1H, ArH), 7.46–7.40 (m, 1H, ArH), 4.36 (d, J = 7.0 Hz, 2H, N-CH_2), 3.16 (t, J = 7.2 Hz, 2H, S-CH_2), 2.39–2.27 (m, 1H, CH), 1.82–1.68 (m, 2H, CH_2), 1.03 (t, J = 7.3 Hz, 3H, CH_3), 0.92 (d, J = 6.7 Hz, 6H, 2-CH_3). ^{13}C NMR (100 MHz, DMSO-d_6) δ 153.3, 151.5, 149.4, 146.4, 136.8, 124.2, 121.8, 119.9, 52.9, 32.3, 28.5, 22.4, 19.7, 13.3. HR-MS (ESI): Calcd. $C_{17}H_{22}N_8S$, $[M+Na]^+$m/z: 393.1580, found: 393.1581.

*4.5.27 3-cyclopropyl-5-(propylthio)-7-(2-(pyridin-2-ylmethylene)hydrazinyl)-3H-[1,2,3]triazolo[4,5-d]pyrimidine (**31**)*

White solid, yield: 89%; m.p.: 203–205 °C. IR (KBr) cm^{-1}, 3165 (NH), 3025 (CH-Ar), 2958 (CH), 2926 (CH), 2865 (CH), 1562 (C=N). ^{1}H NMR (400 MHz, DMSO-d_6) δ 12.59 (s, 1H, NH), 8.62 (d, J = 4.5 Hz, 1H, ArH), 8.31 (s, 1H, N=CH), 8.24–8.15 (m, 1H, ArH), 7.93 (t, J = 7.4 Hz, 1H, ArH), 7.47–7.37 (m, 1H, ArH), 3.95 (m, 1H, N-CH), 3.17 (t, J = 7.2 Hz, 2H, S-CH_2), 1.83–1.71 (m, 2H, cyclopropyl CH_2), 1.35 (d, J = 3.2 Hz, 2H, cyclopropyl CH_2), 1.25–1.19 (m, 2H, CH_2), 1.04 (t, J = 7.3 Hz, 3H, CH_3). ^{13}C NMR (100 MHz, DMSO-d_6) δ 153.3, 149.5, 146.4, 136.8, 128.6, 124.2, 122.1, 119.9, 32.4, 28.1, 22.4, 13.3, 5.8. HR-MS (ESI): Calcd. $C_{16}H_{18}N_8S$, $[M+Na]^+$m/z: 377.1267, found: 377.1266.

*4.5.28 3-cyclopentyl-5-(propylthio)-7-(2-(pyridin-2-ylmethylene)hydrazinyl)-3H-[1,2,3]triazolo[4,5-d]pyrimidine (**32**)*

White solid, yield: 84%; m.p.: 207–208 °C. IR (KBr) cm^{-1}, 3120 (NH), 3055 (CH-Ar), 2954 (CH), 2864 (CH), 1562 (C=N). ^{1}H NMR (400 MHz, DMSO-d_6) δ 12.61 (s, 1H, NH), 8.62 (d, J = 4.5 Hz, 1H, ArH), 8.30 (s, 1H, N=CH), 8.26–8.18 (m, 1H, ArH), 7.94 (t, J = 7.5 Hz, 1H,

ArH), 7.45–7.40 (m, 1H, ArH), 5.29–5.20 (m, 1H, N-CH), 3.16 (t, J = 7.2 Hz, 2H, S-CH_2), 2.29–2.14 (m, 4H, cyclopentyl CH_2), 1.99–1.89 (m, 2H, CH_2), 1.82–1.69 (m, 4H, cyclopentyl CH_2), 1.03 (t, J = 7.3 Hz, 3H, CH_3). ^{13}C NMR (100 MHz, DMSO-d_6) δ 153.3, 150.7, 149.4, 146.3, 136.8, 124.2, 122.3, 119.9, 58.5, 32.3, 31.8, 24.2, 22.4, 13.3. HR-MS (ESI): Calcd. $C_{18}H_{22}N_8S$, $[M+Na]^+$m/z: 405.1580, found: 405.1583.

*4.5.29 3-hexyl-5-(propylthio)-7-(2-(pyridin-2-ylmethylene)hydrazinyl)-3H-[1,2,3]triazolo[4,5-d]pyrimidine (**33**)*

Yellow solid, yield: 75%; m.p.: 167–168 °C. IR (KBr) cm^{-1}, 3149 (NH), 3049 (CH-Ar), 2959 (CH), 2930 (CH), 2861 (CH), 1561 (C=N). ^{1}H NMR (400 MHz, DMSO-d_6) δ 12.62 (s, 1H, NH), 8.62 (d, J = 4.6 Hz, 1H, ArH), 8.32 (s, 1H, N=CH), 8.26–8.17 (m, 1H, ArH), 7.94 (t, J = 7.3 Hz, 1H, ArH), 7.47–7.38 (m, 1H, ArH), 4.53 (t, J = 6.8 Hz, 2H, N-CH_2), 3.16 (t, J = 7.2 Hz, 2H, S-CH_2), 1.99–1.89 (m, 2H, CH_2), 1.82–1.70 (m, 2H, CH_2), 1.32–1.21 (m, 6H, CH_2), 1.03 (t, J = 7.3 Hz, 3H, CH_3), 0.83 (t, J = 7.0 Hz, 3H, CH_3). ^{13}C NMR (100 MHz, DMSO-d_6) δ 168.6, 153.3, 151.0, 149.4, 146.4, 136.8, 124.2, 119.9, 45.9, 32.3, 30.4, 28.5, 25.5, 22.4, 21.8, 13.8, 13.3. HR-MS (ESI): Calcd. $C_{19}H_{26}N_8S$, $[M+Na]^+$m/z: 421.1893, found: 421.1891.

*4.5.30 3-heptyl-5-(propylthio)-7-(2-(pyridin-2-ylmethylene)hydrazinyl)-3H-[1,2,3]triazolo[4,5-d]pyrimidine (**34**)*

Brown solid, yield: 71%; m.p.: 152–155 °C. IR (KBr) cm^{-1}, 3121 (NH), 3021 (CH-Ar), 2965 (CH), 2927 (CH), 2855 (CH), 1562 (C=N). ^{1}H NMR (400 MHz, DMSO-d_6) δ 12.62 (s, 1H, NH), 8.62 (d, J = 4.4 Hz, 1H, ArH), 8.31 (s, 1H, N=CH), 8.25–8.17 (m, 1H, ArH), 7.94 (t, J = 7.4 Hz, 1H, ArH), 7.47–7.38 (m, 1H, ArH), 4.53 (t, J = 6.8 Hz, 2H, N-CH_2), 3.16 (t, J = 7.2 Hz, 2H S-CH_2), 1.99–1.88 (m, 2H, CH_2), 1.81–1.71 (m, 2H, CH_2), 1.30–1.21 (m, 8H, CH_2), 1.02 (t, J = 7.3 Hz, 3H, CH_3), 0.83 (t, J = 6.8 Hz, 3H, CH_3). ^{13}C NMR (100 MHz, DMSO-d_6) δ 178.4, 153.3, 149.5, 136.8, 131.6, 128.6, 124.5, 119.9, 45.9, 31.0, 28.5, 27.9, 25.8, 22.4, 21.9, 13.8, 13.3, 10.8. HR-MS (ESI): Calcd. $C_{20}H_{28}N_8S$, $[M+Na]^+$m/z: 435.2050, found: 435.2052.

5. Materials and methods

5.1 Materials

RPMI-1640, DMEM medium and Fetal Bovine Serum (FBS) were obtained from Hyclone Laboratories (Utah, USA). ERK, p-ERK, AKT, p-AKT, EGFR, JNK, p-JNK, p-P38, Bcl-2, Bid and Caspase-8/9 antibodies were purchased from Cell Signaling Technologies (CST); Bax, P53, PARP, Prx IV-VI and Caspase 3 were purchased from Proteintech (Wuhan, China). Rabbit monoclonal antibodies against Prx I-III were from Epitomics (Hangzhou, China); Annexin V-FITC/PI Apoptosis Detection Kit was purchased from Keygen Biotech. 3-(4,5-dimethylthiazol-2-yl)-2,5-diphenyltetrazolium bromide (MTT) was obtained from Solarbio (China). ROS assay kit, Hoechst 33342 and NAC (N-acetyl-L-cysteine) were purchased from Beyotime Biotechnology. All compounds were dissolved in DMSO to make a 10 mM stock solution.

5.2 Cell culture

Human esophageal carcinoma cell line EC9706, human gastric carcinoma cell line MGC-803, prostate carcinoma cell line PC3 human lung carcinoma cell lines PC9 and liver carcinoma cell line SMMC-7721 were obtained from Cell Bank of the Chinese Academy of Sciences (Shanghai, China). Human esophageal carcinoma cell line KYSE-70 and human immortalized normal esophageal epithelial cell line Het-1A were obtained as gifts from the First Affiliated Hospital of Zhengzhou University, which was purchased from the American Type Culture Collection (Manassas, VA). Human gastric epithelial mucosa cell line GES-1 was purchased from the State Key Laboratory of Molecular Oncology, Chinese Academy of Medical Sciences (Beijing, China). Human normal liver L02 cell line was purchased from Shanghai Institute of Cell Line Bank. Cells were cultured with RPMI-1640 or DMEM medium supplemented with 10% Fetal Bovine Serum (FBS) at 37 °C in a 5% CO_2 humidified atmosphere.

5.3 MTT assay

Based on the growth rate of different cell lines, cells were seeded into 96-well plates at a concentration of 2~5 × 10^3 cells per well. Then, they were treated with serial dilutions of compounds and cultured for 72 h or 1~7 days. Subsequently, 20 μL of MTT solution (5 mg/mL in PBS) was added into each well. The plates were incubated at 37 °C for another 4 h. After adding 150 μL DMSO in each well, followed by removing the MTT, the plates were shaken to dissolve the dark blue crystal (formazan) for 10 minutes and measured at the absorbance of 490

nm. The data were analyzed using SPSS 20 software.

5.4 Colony formation assay

Cells were seeded into 6-well plates at a concentration of 1×10^3 cells per well, followed by treatment with fresh media containing serial dilutions of compounds (0, 12.5, 25, 50 nM for PC3; 0, 25, 50, 100 nM for PC9). After 7 days of incubation, the cells were fixed with 75% ethanol, stained with 0.1% crystal violet solution and then imaged by microscopy (Nikon). After that, the crystal violet crystals were dissolved by ethyl alcohol and measured by a BioTek microplate reader at the absorbance of 595 nm. The data were analyzed using the GraphPad Prism 5 software.

5.5 Analysis of cellular apoptosis

For cell morphology analysis and Hoechst 33342 staining, PC3 and PC9 cells were seeded in 6-well plates at a concentration of $3\sim5 \times 10^5$ cells/well and incubated overnight for adherent, followed by treatment with (0, 25, 50, 100 nM for PC3; 0, 50, 100, 200 nM for PC9) **34** for 72 h. Next, cells were stained with Hoechst 33342 for 30 minutes at room temperature and examined under Nikon Eclipse TE 2000-S fluorescence microscope.

For analysis of apoptosis by flow cytometry, PC3 and PC9 cells were seeded in 6-well plates ($3\sim5 \times 10^5$ cells/well) and incubated overnight. Then, they were treated with different concentrations (0, 12.5, 25, 50, 100, 200 nM for PC3; 0, 50, 100, 200, 400, 800 nM for PC9) of **34** for 72 h. After that, cells were collected and stained with FITC and propidium iodide (PI) for 30 minutes prior to analysis by a flow cytometer. The data were analyzed by FlowJo-V10 and GraphPad Prism 5 software.

5.6 Analysis of intracellular ROS

For the analysis of ROS by flow cytometry, cells were firstly seeded into 6-well plates ($1\sim2\times10^6$ cells/well) and incubated overnight. Then, serial dilutions (0, 12.5, 25, 50, 100, 200 nM for PC3; 0, 50, 100, 200, 400, 800 nM for PC9) of candidate compound **34** were added. After treatment for 72 h, cells were harvested and stained using a cell-based ROS assay kit for 30 minutes. Next, cells were collected and measured by FACSCalibur flow cytometer (BD

Biosciences). All data were analyzed by FlowJo-V10 and GraphPad Prism 5 software.

5.7 LSD1 inhibiory evaluation

Full length LSD1 cDNA encoding LSD1 was obtained by RT-PCR, then cloned into pET-28b. The prepared plasmid pET-28b-LSD1 was then transfected into BL21 (DE). The recombinant was treated with 0.25 mM IPTG at 20 ℃ followed by purification with affinity chromatography, ion exchange chromatography and gel filtration. Then the compounds were incubated with the 5 nM recombinant LSD1 and 25 mM H3K4me2 peptide in the present of FAD (50 nM), Amplex Red (20 nM) and horseradish perosidase (5.5 U/ mL) for 30 min. After that, the fluorescence was measured at excitation wavelength 530 nm and emission wavelength 590 nm as reported in order to evaluate the inhibition rate of the candidate compounds

5.8 Western Blot analysis

PC3 and PC9 cells were seeded in 100 mm^2 plastic dishes (1×10^6 cells/well) and incubated overnight, followed by (0, 25, 50, 100 nM for PC3; 0, 100, 200, 400 nM for PC9) **34** treatment for 72 h. Then, cells were harvested and lysed with RIPA lysis buffer, containing protease inhibitor cocktail for 30 minutes. Next, the buffer was centrifuged at 12 000 r for 20 min at 4 °C. After that, the supernatant was measured by a BCA Protein Assay kit and denatured at 100 °C for 10 min. Subsequently, total proteins were separated by 8%~12% SDS-PAGE, transferred to 0.22 μm nitrocellulose membranes and blocked by 5% skim milk. After being probed with the appropriate primary antibodies at 4 ℃ overnight, the membranes were washed with PBST, followed by the treatment of horseradish-peroxidase-conjugated secondary antibody at room temperature for 2 h. Then, the membranes were washed with PBST again and examined by enhanced chemiluminescence. The data were analyzed using Image J and GraphPad Prism 5 software.

5.9 Statistical analysis

Data were expressed as mean ± standard deviation. Statistical differences were performed using student t-test for two groups comparison and One-Way ANOVA for multiple groups comparison. $P < 0.05$ was considered statistically significant.

Acknowledgement

This work was supported by National Natural Science Foundation of China (Project No. 81438005 and No. 81773562, for H.-M. L.); National Key Research Program of Proteins (No. SQ2018YFE011359 and No. 2016YFA0501800, for H.-M. L. and W. Z); Key Research Program of Henan Province (No. 1611003110100, for H.-M. L.) and Henan Scientific Innovation Talent Team, Department of Education (19IRTSTHN001 by W. Z).

Appendix A. Supplementary data

Supplementary data related to this article can be found at https://doi.org/10.1016/j.bioorg.2020.XXXXXX.

References

[1] World Cancer Report: Cancer Research for Cancer Prevention, WHO, 2020.
[2] R.L. Siegel, K.D. Miller, A. Jemal, Cancer statistics, 2020, CA Cancer J Clin, 70 (2020) 7-30.
[3] A. Bjartell, New Hope in Prostate Cancer Precision Medicine? miRNA Replacement and Epigenetics, Clinical Cancer Research, 25 (2019) 2679.
[4] R.L. Siegel, K.D. Miller, A. Jemal, Cancer statistics, 2019, CA Cancer J Clin, 69 (2019) 7-34.
[5] F. Di Virgilio, E. Adinolfi, Extracellular purines, purinergic receptors and tumor growth, Oncogene, 36 (2016) 293.
[6] L.-H. Huang, H.-D. Xu, Z.-Y. Yang, Y.-F. Zheng, H.-M. Liu, Synthesis and anticancer activity of novel C6-piperazine substituted purine steroid–nucleosides analogues, Steroids, 82 (2014) 1-6.
[7] U. Pradère, V. Roy, A. Montagu, O. Sari, M. Hamada, J. Balzarini, R. Snoeck, G. Andrei, L.A. Agrofoglio, Synthesis and antiviral evaluation of bis(POM) prodrugs of (E)-[4′-phosphono-but-2′-en-1′-yl]purine nucleosides, Eur J Med Chem, 57 (2012) 126-133.
[8] G. Burnstock, Purinergic signalling and disorders of the central nervous system, Nature Reviews Drug Discovery, 7 (2008) 575.
[9] L.J.S. Knutsen, J. Lau, H. Petersen, C. Thomsen, J.U. Weis, M. Shalmi, M.E. Judge, A.J. Hansen, M.J. Sheardown, N-Substituted Adenosines as Novel Neuroprotective A1 Agonists with Diminished Hypotensive Effects, J Med Chem, 42 (1999) 3463-3477.
[10] J.A. Montgomery, T.P. Johnston, A. Gallagher, C.R. Stringfellow, F.M. Schabel, A Comparative Study of the Anticancer Activity of Some S-Substituted Derivatives of 6-Mercaptopurine and their Ribonucleosides, J Med Pharm Chem, 3 (1961) 265-288.
[11] P. Podsiadlo, V.A. Sinani, J.H. Bahng, N.W.S. Kam, J. Lee, N.A. Kotov, Gold Nanoparticles Enhance the Anti-Leukemia Action of a 6-Mercaptopurine Chemotherapeutic Agent, Langmuir, 24 (2008) 568-574.
[12] C.W. Noell, R.K. Robins, The Antitumor Activity of 2-Amino-6-alkylthio-9-(β-D-ribofuranosylpurines and related Derivatives of 2-Amino-6-purinethiol (Thioguanine), J Med Pharm

Chem, 5 (1962) 1074-1085.
[13] S. Husted, J.J.J. Van Giezen, Ticagrelor: The First Reversibly Binding Oral P2Y12 Receptor Antagonist, Cardiovasc Ther, 27 (2009) 259-274.
[14] R.J. Gillespie, S.J. Bamford, R. Botting, M. Comer, S. Denny, S. Gaur, M. Griffin, A.M. Jordan, A.R. Knight, J. Lerpiniere, S. Leonardi, S. Lightowler, S. McAteer, A. Merrett, A. Misra, A. Padfield, M. Reece, M. Saadi, D.L. Selwood, G.C. Stratton, D. Surry, R. Todd, X. Tong, V. Ruston, R. Upton, S.M. Weiss, Antagonists of the Human A2A Adenosine Receptor. 4. Design, Synthesis, and Preclinical Evaluation of 7-Aryltriazolo[4,5-d]pyrimidines, J Med Chem, 52 (2009) 33-47.
[15] A. Gigante, M.-D. Canela, L. Delang, E.-M. Priego, M.-J. Camarasa, G. Querat, J. Neyts, P. Leyssen, M.-J. Pérez-Pérez, Identification of [1,2,3]Triazolo[4,5-d]pyrimidin-7(6H)-ones as Novel Inhibitors of Chikungunya Virus Replication, J Med Chem, 57 (2014) 4000-4008.
[16] Z. Li, L. Ding, Z. Li, Z. Wang, F. Suo, D. Shen, T. Zhao, X. Sun, J. Wang, Y. Liu, L. Ma, B. Zhao, P. Geng, B. Yu, Y. Zheng, H. Liu, Development of the triazole-fused pyrimidine derivatives as highly potent and reversible inhibitors of histone lysine specific demethylase 1 (LSD1/KDM1A), Acta Pharmaceutica Sinica B, 9 (2019) 794-808.
[17] C.M. Dehnhardt, A.M. Venkatesan, E. Delos Santos, Z. Chen, O. Santos, S. Ayral-Kaloustian, N. Brooijmans, R. Mallon, I. Hollander, L. Feldberg, J. Lucas, I. Chaudhary, K. Yu, J. Gibbons, R. Abraham, T.S. Mansour, Lead Optimization of N-3-Substituted 7-Morpholinotriazolopyrimidines as Dual Phosphoinositide 3-Kinase/Mammalian Target of Rapamycin Inhibitors: Discovery of PKI-402, J Med Chem, 53 (2010) 798-810.
[18] F. Trausel, C. Maity, J.M. Poolman, D.S.J. Kouwenberg, F. Versluis, J.H. van Esch, R. Eelkema, Chemical signal activation of an organocatalyst enables control over soft material formation, Nat Commun, 8 (2017) 879.
[19] P. Kodisundaram, S. Amirthaganesan, T. Balasankar, Antimicrobial Evaluation of a Set of Heterobicyclic Methylthiadiazole Hydrazones: Synthesis, Characterization, and SAR Studies, J Agric Food Chem, 61 (2013) 11952-11956.
[20] J. Amato, R. Morigi, B. Pagano, A. Pagano, S. Ohnmacht, A. De Magis, Y.-P. Tiang, G. Capranico, A. Locatelli, A. Graziadio, A. Leoni, M. Rambaldi, E. Novellino, S. Neidle, A. Randazzo, Toward the Development of Specific G-Quadruplex Binders: Synthesis, Biophysical, and Biological Studies of New Hydrazone Derivatives, J Med Chem, 59 (2016) 5706-5720.
[21] O.I. El-Sabbagh, H.M. Rady, Synthesis of new acridines and hydrazones derived from cyclic β-diketone for cytotoxic and antiviral evaluation, Eur J Med Chem, 44 (2009) 3680-3686.
[22] C.M. Moldovan, O. Oniga, A. Pârvu, B. Tiperciuc, P. Verite, A. Pîrnău, O. Crişan, M. Bojiţă, R. Pop, Synthesis and anti-inflammatory evaluation of some new acyl-hydrazones bearing 2-aryl-thiazole, Eur J Med Chem, 46 (2011) 526-534.
[23] D.A. Rodrigues, G.À. Ferreira-Silva, A.C.S. Ferreira, R.A. Fernandes, J.K. Kwee, C.M.R. Sant'Anna, M. Ionta, C.A.M. Fraga, Design, Synthesis, and Pharmacological Evaluation of Novel N-Acylhydrazone Derivatives as Potent Histone Deacetylase 6/8 Dual Inhibitors, J Med Chem, 59 (2016) 655-670.
[24] V. Sorna, E.R. Theisen, B. Stephens, S.L. Warner, D.J. Bearss, H. Vankayalapati, S. Sharma, High-Throughput Virtual Screening Identifies Novel N′-(1-Phenylethylidene)-benzohydrazides as Potent, Specific, and Reversible LSD1 Inhibitors, J Med Chem, 56 (2013) 9496-9508.
[25] Z.-H. Li, X.-Q. Liu, T.-Q. Zhao, P.-F. Geng, W.-G. Guo, B. Yu, H.-M. Liu, Design, synthesis and preliminary biological evaluation of new [1,2,3]triazolo[4,5-d]pyrimidine/thiourea hybrids as

antiproliferative agents, Eur J Med Chem, 139 (2017) 741-749.
[26] Z.-H. Li, X.-Q. Liu, P.-F. Geng, F.-Z. Suo, J.-L. Ma, B. Yu, T.-Q. Zhao, Z.-Q. Zhou, C.-X. Huang, Y.-C. Zheng, H.-M. Liu, Discovery of [1,2,3]Triazolo[4,5-d]pyrimidine Derivatives as Novel LSD1 Inhibitors, ACS Med Chem Lett, 8 (2017) 384-389.
[27] P.-F. Geng, X.-Q. Liu, T.-Q. Zhao, C.-C. Wang, Z.-H. Li, J. Zhang, H.-M. Wei, B. Hu, L.-Y. Ma, H.-M. Liu, Design, synthesis and in vitro biological evaluation of novel [1,2,3]triazolo[4,5-d]pyrimidine derivatives containing a thiosemicarbazide moiety, Eur J Med Chem, 146 (2018) 147-156.
[28] K. Sun, J.-D. Peng, F.-Z. Suo, T. Zhang, Y.-D. Fu, Y.-C. Zheng, H.-M. Liu, Discovery of tranylcypromine analogs with an acylhydrazone substituent as LSD1 inactivators: Design, synthesis and their biological evaluation, Bioorg Med Chem Lett, 27 (2017) 5036-5039.
[29] L.-Y. Li, J.-D. Peng, W. Zhou, H. Qiao, X. Deng, Z.-H. Li, J.-D. Li, Y.-D. Fu, S. Li, K. Sun, H.-M. Liu, W. Zhao, Potent hydrazone derivatives targeting esophageal cancer cells, Eur J Med Chem, 148 (2018) 359-371.
[30] L.K. Gediya, V.C.O. Njar, Promise and challenges in drug discovery and development of hybrid anticancer drugs, Expert Opin Drug Discov, 4 (2009) 1099-1111.
[31] V.-J. Claudio, D. Amanda, B. Vanderlan da Silva, J.B. Eliezer, F. Carlos Alberto Manssour, Molecular Hybridization: A Useful Tool in the Design of New Drug Prototypes, Curr Med Chem, 14 (2007) 1829-1852.
[32] P.T. Schumacker, Reactive oxygen species in cancer cells: Live by the sword, die by the sword, Cancer Cell, 10 (2006) 175-176.
[33] P.D. Ray, B.-W. Huang, Y. Tsuji, Reactive oxygen species (ROS) homeostasis and redox regulation in cellular signaling, Cell Signal, 24 (2012) 981-990.
[34] M.S. Mady, M.M. Mohyeldin, H.Y. Ebrahim, H.E. Elsayed, W.E. Houssen, E.G. Haggag, R.F. Soliman, K.A. El Sayed, The indole alkaloid meleagrin, from the olive tree endophytic fungus Penicillium chrysogenum, as a novel lead for the control of c-Met-dependent breast cancer proliferation, migration and invasion, Bioorg Med Chem, 24 (2016) 113-122.
[35] S. Dadashpour, S. Emami, Indole in the target-based design of anticancer agents: A versatile scaffold with diverse mechanisms, Eur J Med Chem, 150 (2018) 9-29.
[36] X.-J. Shi, L. Ding, W. Zhou, Y. Ji, J. Wang, H. Wang, Y. Ma, G. Jiang, K. Tang, Y. Ke, W. Zhao, H.-M. Liu, Pro-Apoptotic Effects of JDA-202, a Novel Natural Diterpenoid, on Esophageal Cancer Through Targeting Peroxiredoxin I, Antioxid Redox Signal, 27 (2016) 73-92.
[37] L. Chen, W. Fu, L. Zheng, Z. Liu, G. Liang, Recent Progress of Small-Molecule Epidermal Growth Factor Receptor (EGFR) Inhibitors against C797S Resistance in Non-Small-Cell Lung Cancer, J Med Chem, 61 (2018) 4290-4300.
[38] O.M. AboulWafa, H.M.G. Daabees, W.A. Badawi, 2-Anilinopyrimidine derivatives: Design, synthesis, in vitro anti-proliferative activity, EGFR and ARO inhibitory activity, cell cycle analysis and molecular docking study, Bioorg Chem, 99 (2020) 103798.
[39] L.M. Ellis, Epidermal growth factor receptor in tumor angiogenesis, Hematol Oncol Clin North Am, 18 (2004) 1007-1021.